DISSERTATIONES
CHIMICAE
UNIVERSITATIS
TARTUENSIS
206

ELIISE TAMMEKIVI

Derivatization and quantitative gas-chromatographic analysis of oils

DISSERTATIONES CHIMICAE UNIVERSITATIS TARTUENSIS
206

DISSERTATIONES CHIMICAE UNIVERSITATIS TARTUENSIS
206

ELIISE TAMMEKIVI

Derivatization and quantitative gas-chromatographic analysis of oils

UNIVERSITY OF TARTU
Press

Institute of Chemistry, Faculty of Science and Technology, University of Tartu, Estonia

Dissertation is accepted for the commencement of the degree of *Doctor philosophiae* in Chemistry on June 18th, 2021 by the Council of Institute of Chemistry, Faculty of Science and Technology, University of Tartu

Supervisors:	Prof. Ivo Leito (PhD), Research Fellow Signe Vahur (PhD) Institute of Chemistry, University of Tartu, Estonia
Opponent:	Dr. Gregory Dale Smith (PhD), Indianapolis Museum of Art, USA
Commencement:	August 27th, 2021 at 16.15, Ravila 14A–1020, Tartu (Chemicum) and Microsoft Teams (*online*)

Publication of this dissertation is granted by University of Tartu, Estonia.

This work has been partially supported by Graduate School of Functional materials and technologies receiving funding from the European Regional Development Fund in University of Tartu, Estonia.

ISSN 1406-0299
ISBN 978-9949-03-636-3 (print)
ISBN 978-9949-03-637-0 (pdf)

University of Tartu Press
www.tyk.ee

TABLE OF CONTENTS

LIST OF ORIGINAL PUBLICATIONS

This thesis is based on the following three publications. In the text, these are referred to as paper I, paper II, and paper III.

I. **Tammekivi, E.**; Vahur, S.; Kekišev, O.; van der Werf, I. D.; Toom, L.; Herodes, K.; Leito, I. Comparison of derivatization methods for the quantitative gas chromatographic analysis of oils. *Analytical Methods*, **2019**, *11* (28), 3514–3522. DOI:10.1039/c9ay00954j.

II. Vilbaste, M.; **Tammekivi, E.**; Leito, I. Uncertainty contribution of derivatization in gas chromatography/mass spectrometric analysis. *Rapid Communications in Mass Spectrometry*, **2020**, *34* (16), e8704. DOI: 10.1002/rcm.8704.

III. **Tammekivi, E.**; Vahur, S.; Vilbaste, M.; Leito, I. Quantitative GC-MS analysis of artificially aged paints with variable pigment and linseed oil ratios. *Molecules*, **2021**, *26* (8), 2218. DOI: 10.3390/molecules26082218.

Author's contribution

Paper I. Lead author in preparing the manuscript. Performed all the experiments (excluding quantitative NMR).

Paper II. Performed all experiments. Participated in the writing of the manuscript.

Paper III. Lead author in preparing the manuscript. Performed all the experiments (excluding the preparation and aging of the paint mock-ups).

ABBREVIATIONS

∑D	the sum of the relative content of dicarboxylic acids
A/P	azelaic acid to stearic acid ratio
ACM	acid-catalyzed methylation
ATR	attenuated total reflection
BSTFA	*N*,*O*-bis(trimethylsilyl)trifuoroacetamide
$CDCl_3$	deuterated chloroform
DCM	dichloromethane
EE	ethyl ester
FAEES	fatty acid ethyl esters
FAME	fatty acid methyl ester
FID	flame ionization detector
FT-IR	Fourier transform infrared
GC	gas chromatography
GUM	Guide to the Expression of Uncertainty in Measurement
IS	internal standard
k	coverage factor
m/z	mass-to-charge ratio
MCM	Monte Carlo method
ME	methyl ester
MS	mass spectrometry
MTBSTFA	methyltributylsilyl tetrafluoroacetamine
NaOEt	sodium ethoxide
NMR	nuclear magnetic resonance
P/S	palmitic acid to stearic acid ratio
PDF	probability density function
qNMR	quantitative nuclear magnetic resonance
R	derivatization efficiency (yield)
RH	relative humidity
SIM	selected ion monitoring
TAG	triacylglyceride
TBDMS	*tert*-butyldimethylsilyl derivative
TIC	total ion chromatogram
TMS	tetramethylsilane
TMSE	trimethylsilyl ester
TMTFTH	m-(-trifluoromethyl)phenyltrimethylammonium hydroxide
t_R	retention time
u_c	combined standard uncertainty

1. INTRODUCTION

For centuries, vegetable oils have been used in various areas such as nutrition, art, skin and cosmetic products, medicine, and fuel. These oils are obtained from plant sources like vegetables, seeds, or nuts. Depending on their chemical and physical properties, different oils have been used for various purposes – for example, canola and olive oil for cooking, almond oil in cosmetics, castor oil as biodiesel, etc. However, for making paints, oils that form a solid layer while binding together all other paint components (so-called drying oils) must be used. The most common drying oils used as binders are linseed, poppy, and walnut oils. The analysis of these vegetable oils may have numerous objectives. For example, the analysis of cooking oils is performed to determine their nutritional value, adulterations, evaluate the influence of heating, or establish the oil's quality by analyzing minor components. Because vegetable oils are a renewable resource that are widely used in many products, the need for accurate and comprehensive analysis is expected to increase.

In cultural heritage, the analysis of oil-based binders is needed to characterize and identify the materials used to paint and/or protect an artifact. However, the chemical composition of oils used in art changes during the aging of an oil-based paint, which complicates the identification of the original material. The identification of oil binders has some unresolved questions, such as how to unravel the raw materials in a mixture of similar compounds or differentiate between traditional and modern oil paints. Also, because of the degradation processes, the properties of the binder change that may cause the paint to turn yellow, crack, develop deposits on the paint surface, become more sensitive to water, etc. Therefore, the chemical composition of the paint and degradation processes need to be studied to choose suitable conservation procedures, materials, and storage conditions to maintain the object's visual appearance. Often qualitative analysis of characteristic compounds or degradation products is used. However, in the case of materials with similar composition (including oils used for painting), quantitative analysis is used more and more for the identification and observation of the degradation processes.

One of the most widely applied methods to analyze oils is gas chromatography (GC) combined with derivatization. A wide range of derivatization methods have been used, including reagents performing acid- and base-catalyzed alkylations, silylation, and transesterification. However, all these procedures are rarely 100% efficient in derivatizing the triglyceride molecules present in vegetable oils. Moreover, their efficiency and the associated uncertainty have not been comparatively evaluated for the different derivatization methods.

Therefore, the **aims of this thesis** are the following:

1. Compare four widespread derivatization methods used for the GC analysis of oils, including modifications to enable absolute quantification.
2. Realistically assess the uncertainty contribution of the derivatization step.

3. Apply the improved procedures for the analysis of samples from different fields: dried oil paint samples (self-made and from artifacts) and yeast cells.

First, a comprehensive comparison of four derivatization methods (TMTFTH, acid-catalyzed methylation, KOH–BSTFA, and NaOEt–BSTFA) widely used in cultural heritage and archaeology was performed based on the quantitative analysis of fresh oils – canola and linseed oil. Performance parameters – derivatization efficiency (yield) and intermediate precision (within-lab reproducibility) – together with experimental characteristics – time and cost of analysis, sample preparation, and complexity of interpretation – were evaluated. The results present the most suitable derivatization method for the absolute quantification of the studied fresh vegetable oils.

Although derivatization is a widely used step in the GC and high-performance liquid chromatography (HPLC) analyses, specifically, the uncertainty contribution of the derivatization part has not been studied in detail. Therefore, the second step of this thesis was to apply two bottom-up uncertainty estimation approaches – the traditional GUM and the Monte Carlo method (MCM) – to estimate the uncertainty of derivatization. This study proposes the preferred uncertainty estimation approach and discusses the aspects of uncertainty estimation of derivatization.

Finally, in the third step, a suitable derivatization method and the improved quantitative analysis were applied for the analysis of various samples, ranging from cultural heritage to biorefinery. Both relative and absolute quantification were performed on a comprehensive set of self-made artificially aged paint samples with varying pigment to linseed oil ratios. The aim was to study if and how much pigment concentration affects the composition of drying oil and to monitor different ratios, including the palmitic to stearic acid ratio (P/S) that is the most common parameter to distinguish between drying oils. Relative quantification was also used to study two case study samples relevant to the history of Estonia. Finally, the improved absolute quantification procedure was applied for the quantification of triglycerides in lyophilized yeast cells (*Rhodotorula toruloides*). Knowing the absolute fatty acid content in the cell samples is an important step in facilitating the further development and usage of yeast cells to produce lipid-based sustainable chemicals and fuels.

2. LITERATURE OVERVIEW

2.1. Composition of oils

Naturally occurring oils mainly consist of triacylglyceride molecules (TAGs, aka triglycerides), which in turn are made of one glycerol moiety bound via the ester linkages to three fatty acid residues. Besides TAGs, vegetable oils may also contain mono- and diglycerides, free fatty acids, and glycerol in smaller quantities.[1] Traditionally (and in this thesis), the fatty acid residues are called by the name of the corresponding fatty acid for simplicity. Also, wherever only the term "oil" is used, specifically vegetable oils are meant. The fatty acids in TAGs are monocarboxylic acids that usually have an even-numbered linear carbon chain with carbon number ranging from 4 to 24. The fatty acids may be saturated or unsaturated. In one triglyceride molecule, the fatty acids are present in random combinations. The most widespread fatty acids are known by their trivial name and are often abbreviated as CX:Y, where X represents the number of carbon atoms in the aliphatic chain and Y is the number of double bonds. The most abundant fatty acid residues in oils are palmitic (C16:0), stearic (C18:0), oleic (C18:1), linoleic (C18:2), and linolenic (C18:3) acid (see Table 1).[2] For one type of oil, there are no fixed fatty acid percentages because the exact composition of the original oil source depends largely on the geographical origin and meteorological effects.[3]

Table 1. Percentages of fatty acid residues in some of the most common oils.[2,4]

Fatty acid	Vegetable oil (%)				
	Linseed	**Walnut**	**Poppy**	**Canola**	**Olive**
Palmitic acid (C16:0)	4–10	9–11	3–8	3–6	7–16
Stearic acid (C18:0)	2–8	1–2	0.5–3	1–2.5	2–4
Oleic acid (sum of *Z*+*E*) (C18:1)[a]	10–24	11–18	9–30	52–66	64–86
Linoleic acid (C18:2)	12–19	69–77	57–76	17–25	4–15
Linolenic acid (C18:3)	48–60	3–5	2–16	8–11	0.5–1

[a] Often the percentage of C18:1 is expressed as the sum of oleic acid ((*Z*)-Octadec-9-enoic acid) and elaidic acid ((*E*)-Octadec-9-enoic acid).

2.2. Utilization of vegetable oils

For centuries, various vegetable oils such as olive, canola, and coconut oil have been used for cooking, fuel, cosmetics, and for other purposes.[2] In recent years, more and more vegetable oils (including nonedible oils such as castor oil) are used as renewable sources for making biodiesel, stabilizers, lubricants, emulsifiers, agrochemicals, pharmaceuticals, solvents, fragrances, and so on.[5–10] This progress in the last decades demonstrates that oils are also an important starting material for green chemistry.[5] Because of its wide use in food and medical

industries as well as growing use in green chemistry, accurate methods are needed for the chemical analysis of oils. One big problem is the adulteration of oil products.[11–14] For example, chemical analyses are necessary to detect if virgin olive oil has been tampered with cheaper and lower quality seed oils (e.g., hazelnut oil).[11,15] Other aims for the analysis of vegetable oils include the quality or authenticity assessment based on minor compounds[16,17] and studying the impact of heating/frying.[18,19]

The first written sources about using oils as binding materials in paints originate from the 11th–12th century, although there are additional pieces of evidence that using oil binders has a longer history. From the 15th century, oils gradually started to replace the more common egg-based binding medium (tempera). The reason behind the replacement was the more transparent look of the oil-based paint.[20] Since around the 17th century, oils are one of the most used natural binding materials next to proteinaceous materials (egg, casein), waxes (beeswax, carnauba), polysaccharide materials (plant gums), and resins (colophony, shellac).[21] Usually, linseed, poppy, or walnut oil is used as the oil binder. These oils have high levels of polyunsaturated fatty acids (at least 65% of linoleic and linolenic acid), which polymerize due to air oxygen and turn the former liquid oil into a solid layer. Because of that, these oils – called drying oils – are suitable to be used as paint binders.[4,20] Among them, linseed oil dries the fastest (because of the highest linolenic acid concentration) and turns touch-dry in a few days. However, the drying processes of all drying oils continue for many years and are influenced by oil pre-treatments and other paint components (mainly pigments). Linseed oil is the most common drying oil, even though it tends to yellow the most. To overcome yellowing, after extraction from flax seeds, linseed oil can be bleached under sunlight to produce clarified linseed oil, which is often used by artists.[22,23] Poppy oil tends to yellow less and has lower viscosity; however, it takes longer to dry and is more likely to crack or soften after drying.[2] Walnut oil dries longer and is less likely to turn yellow compared to linseed oil. Still, it is seldom used in tube colors for its property to turn easily rancid (nowadays, this problem can be reduced by using alkali-refined walnut oil[4]).[22]

Manufacturing of paints around the start of the 20th century introduced also other oils (besides the traditional drying oils) into the binding media. These include semi-drying oils that contain less unsaturated fatty acids (e.g., canola oil, soybean oil) that can slow down the curing processes. Even non-drying oils (e.g., castor oil, olive oil) have been added to paint mixtures. The usage of semi- and non-drying oils decreased the price of the paint and also made it more stable to be stored in tubes. Nowadays, these are called modern oil paints due to their different composition compared to traditional oil paint and commercial production. Besides oils, other additional compounds may have been added to modern oil paints, such as metal stearates, hydrogenated castor oil, and stabilizing agents.[4,24,25]

In closed containers and at ambient temperature, the drying oils are liquid. However, they start to solidify when laid as a thin layer and left to air dry. The

double bonds in the unstable polyunsaturated fatty acid residues in the TAG molecules react with air oxygen, and highly reactive peroxidic compounds are produced.[23,26] These, in turn, can cause reactions between the carbon chains. The peroxidic groups easily decompose and form free radicals that react with each other. Consequently, the carbon chains are combined via new C–C, C–O–C, or C–O–O–C "bridges", leading to the formation of a cross-linked insoluble polymeric film (Figure 1). The extent of the drying process (also called aging of the oil) decreases in time but may take several months, or even years, as long there are free radicals.[23,26,27]

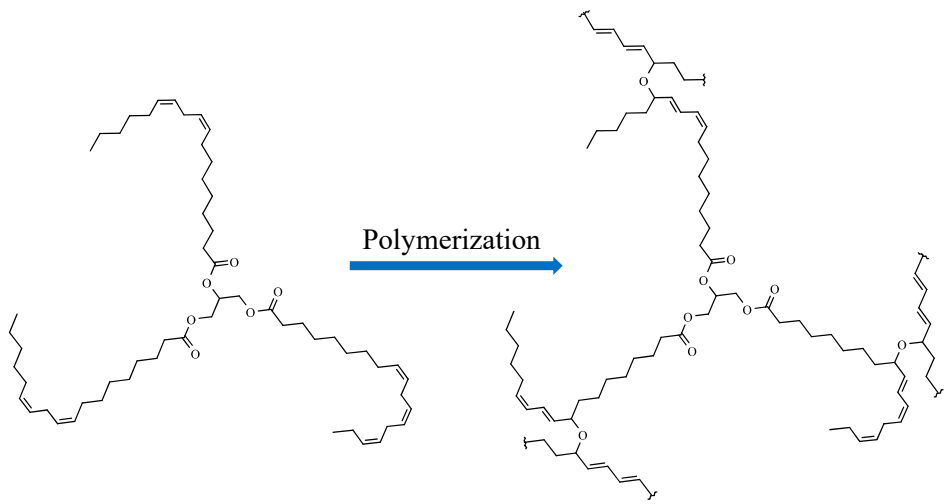

Figure 1. Polymerization of a representative triglyceride.

Besides the formation of a polymeric structure, smaller fragments (ketones, aldehydes, alcohols, dicarboxylic acids) can form as a result of the oxidative cleavage reaction (Figure 2). These compounds may evaporate during the drying of the oil, causing an additional change in its composition.[23] Therefore, the dried oil's chemical composition is very different from the composition of the original fresh oil. Because of the possibility of numerous and complex reaction paths, the exact autooxidation mechanism of a drying oil is not yet fully understood.[28]

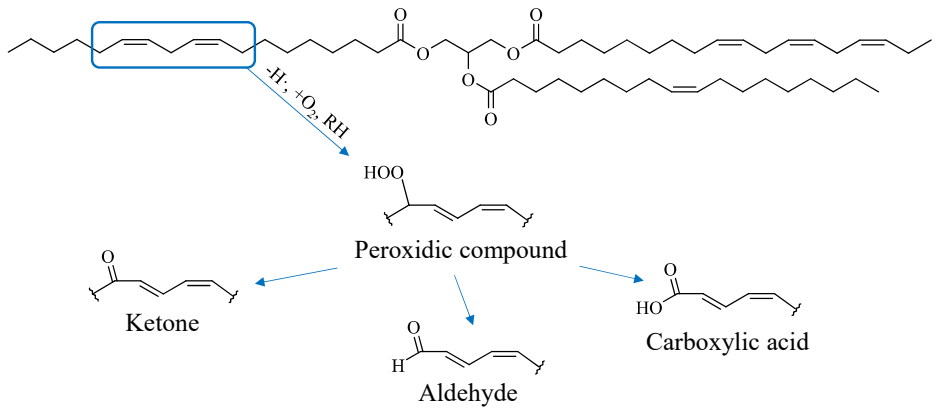

Figure 2. Oxidation of a representative triglyceride. A peroxidic compound is formed by the removal of hydrogen (-H·), reaction with oxygen (+O_2), and water vapor (RH, relative humidity). From this various new compounds can be formed.[23]

The drying process can be accelerated by using various factors such as heat,[28,29] UV light,[30] higher relative humidity (RH),[31,32] or by adding siccatives aka driers.[28] Driers are metal compounds that can speed up the drying of an oil, for example, by decomposing the hydroperoxides and thus increasing the number of free radicals.[33] Some pigments (e.g., burnt umber, cobalt blue, and lead white[28,33–35]) have been shown to act as driers in addition to providing color to the paint.

2.3. Analysis of vegetable oils

Various methods like high-performance liquid chromatography (HPLC),[24,36–40] Fourier transform infrared (FT-IR) spectroscopy,[15,18,41] matrix-assisted laser desorption/ionization mass spectrometry (MALDI-MS),[11,12,42–44] and ultraviolet-visible spectroscopy (UV-Vis)[45–47] have been used for the analysis of vegetable oils. However, for the analysis of oils used in cultural heritage artifacts, by far the most common method is gas chromatography (GC).[48] GC is a type of chromatography where the mobile phase is an inert gas (often He), and the stationary phase is a low volatility liquid on the internal surface of a column. The compounds separate from each other based on differences in boiling points and, to a lesser extent, based on the components' interactions with the stationary phase. GC is a method with high sensitivity and selectivity that enables the analysis of various thermally stable and volatile organic and inorganic compounds with boiling points below 500 °C (in the case of conventional GC systems).[49,50] Compared to spectroscopic methods (IR and UV-Vis) used to analyze oils, GC allows the identification and quantification of analyte(s) in a

mixture of similar compounds using the corresponding standards and/or a mass spectrometric detector (MS). Compared to MALDI mass spectrometry, GC enables a more reliable and robust quantitative analysis of specific compounds, and a GC is more commonly available in laboratories. While HPLC analysis requires the sample to be dissolved in a solvent that is compatible with the eluent, for GC, almost any common solvent (except water) can be used. Also, because of the higher efficiency of GC it is often easier to obtain good separation of the original and degradation products of oils than with HPLC, where development of a successful separation method can be labor-intensive.[51,52] Together with a MS detector, GC-MS is an essential technique used for the separation of complex samples and the identification of the separated compounds. In cultural heritage, besides being the principal analysis technique used for the analysis of lipids, it is also frequently involved as a confirmatory method – often various spectroscopic, chromatographic, and mass spectrometric techniques are used in combination for the full characterization of a sample.[24,48,53] Because TAG molecules in oils are not volatile enough for the GC analysis, derivatization is required to obtain smaller and less polar fragments. By this chemical alteration, it is also possible to improve the thermal stability, detection, and separation of the analytes. In Figure 3, the general scheme for the derivatization of a TAG molecule is presented.

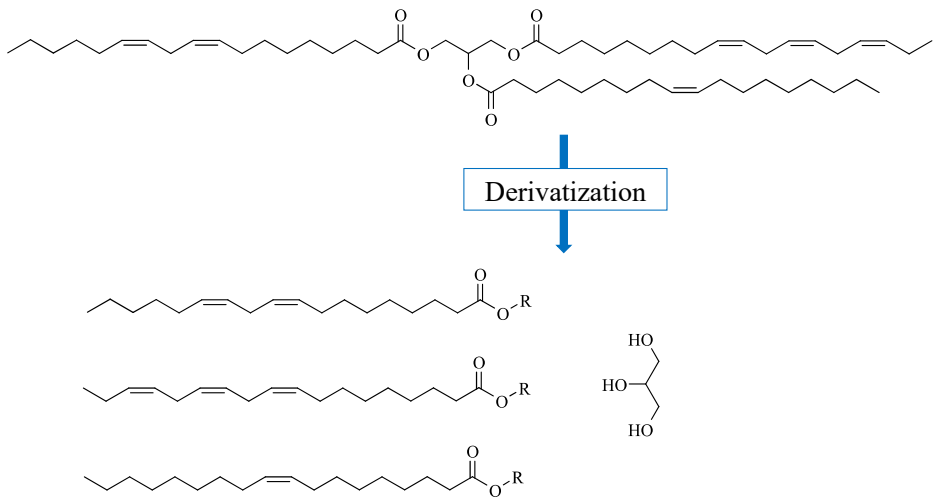

Figure 3. General scheme for the derivatization of a representative TAG molecule.

Since the 1970s–1980s, a wide range of derivatization procedures with different reagents have been developed to analyze oils in art materials and objects.[48] By these procedures, the TAGs are hydrolyzed, and then the fatty acid residues are derivatized mainly to methyl, ethyl, or silyl esters.[21] In recent years mostly silyla-

tion (for example, derivatization with BSTFA: *N*,*O*-bis(trimethylsilyl)trifuoroacetamide, BSA: *N*,*O*-bis(trimethylsilyl)acetamide, or HMDS: hexamethyldisilazane)[54] and transesterification (e.g., acid- or base-catalyzed alkylation, reactions with basic quaternary ammonium reagents) methods are used. The procedures including transesterification are especially convenient because the fatty acids in TAGs are directly alkylated without the hydrolysis step.[55] Even though there are numerous derivatization procedures, only a few studies[56–59] have focused their research on the comparison of the methods.

In paper I, four derivatization methods were compared:

a) **TMTFTH**: TMTFTH (m-(-trifluoromethyl)phenyltrimethylammonium hydroxide, commercially known also as Meth-Prep II) methylation
b) **ACM**: acid-catalyzed methylation
c) **KOH–BSTFA**: saponification with KOH followed by BSTFA trimethylsilylation
d) **NaOEt–BSTFA**: ethylation with sodium ethoxide (NaOEt) and trimethylsilylation with BSTFA

The general reaction schemes for these derivatizations are presented in Figure 4. The first two methods are transesterification reactions, where ACM is a widespread procedure used in archaeology and the more novel TMTFTH derivatization is mainly used in the analysis of art objects.[59] TMTFTH is a quaternary ammonium reagent that combined with the fatty acid residues yields quaternary ammonium salts that decompose under 220–300 °C in the GC inlet to produce methylated fatty acids. This simplifies the sample preparation and has gained popularity for the TMTFTH derivatization, especially for the analysis of small samples obtained from valuable art objects.[60] BSTFA derivatization reagent is even more widely used in cultural heritage, often preceded by various saponification/hydrolysis steps. The NaOEt–BSTFA derivatization yields mainly ethylated derivatives from TAGs and a small amount of trimethylsilyl esters (TMSE) from free fatty acids. Besides their wide use, these four derivatizations methods were chosen because these do not require any special equipment (for example, a pyrolizer[61]) in addition to a standard GC. The well-known tetramethylammonium hydroxide (TMAH) was excluded because this derivatization reagent requires higher temperatures than the conventional GC inlet can provide (>600 °C) and therefore is almost exclusively used with a pyrolysis GC-MS (PyGC-MS) device.[62]

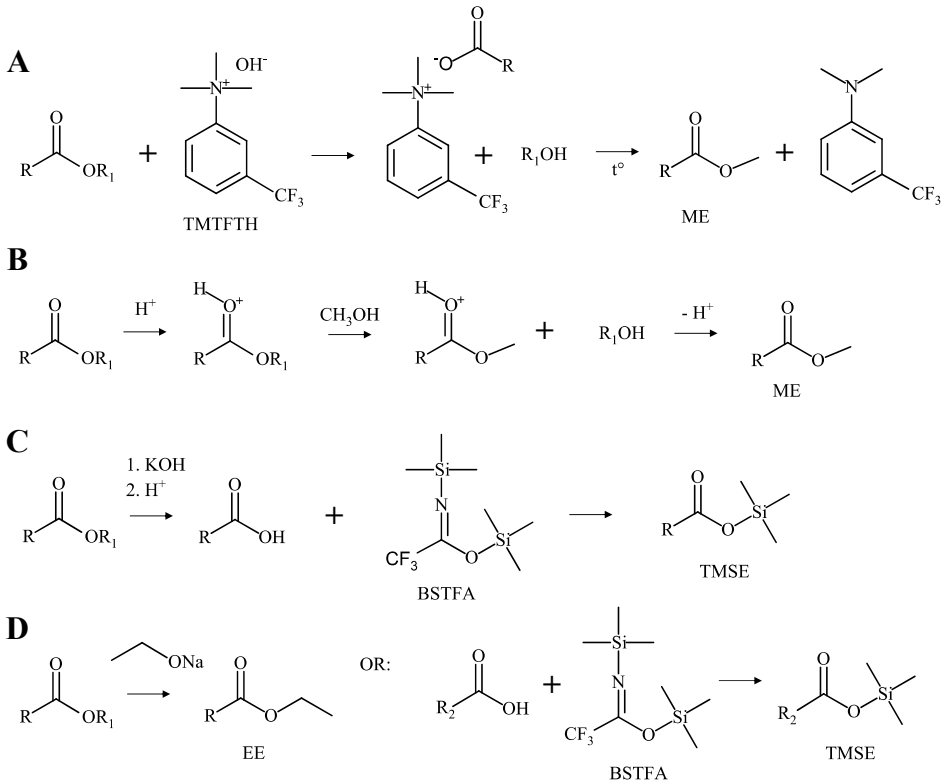

Figure 4. Reaction schemes of **A**: TMTFTH methylation,[4] **B**: ACM derivatization,[63] **C**: KOH–BSTFA derivatization,[64,65] and **D**: NaOEt–BSTFA derivatization.[65] ME – methyl ester, TMSE – trimethylsilyl ester, and EE – ethyl ester.

Both MS and flame ionization detector (FID) were applied in paper I to assess if one has advantages over the other in terms of the quantitative analysis of oils. With the MS detector, the compounds are ionized, the ions are separated by their mass-to-charge (*m/z*) ratio, and mass spectra are recorded at short intervals. The separated compounds can be identified by comparing the recorded mass spectrum to spectra in a library and/or by analyzing a standard of the same compound with the same chromatographic conditions (identification based both on retention times and mass spectra). Practically all compounds that can be separated by the GC can be detected with the MS detector using electron impact ionization. In the case of FID, the separated compounds are burned and ionized in an H_2 flame. The compounds must contain at least one C–C or C–H bond to be detected with FID – a requirement that is easily met with almost all organic compounds. FID is often preferred for quantitative analysis, but identification can only be achieved by analyzing the corresponding standards under the same chromatographic conditions.[49,66,67]

2.4. Characterization of vegetable oils

Several factors complicate the determination of the type of an oil using GC-MS. Identification based on qualitative analysis could be performed based on some specific marker compounds. For example, canola oil can be identified based on the presence of (*Z*)-eicos-11-enoic (gondoic) and (*Z*)-docos-13-enoic (erucic) acid. The same is the case for castor oil, whose presence can be confirmed by identifying ricinoleic acid.[4] However, most oils (including linseed, poppy, and walnut oil) largely consist of the residues of the same five fatty acids (see Table 1). The only variance comes from the fact that the relative quantities of these fatty acid residues are different.[67] Therefore, qualitative analysis is not always enough, and quantitative analysis with GC-MS could be the solution.

Quantitative analysis of fatty acids present in fresh oils could help to distinguish between different oils. However, in the case of aged drying oils, most of the unsaturated fatty acids present in the fresh oil have gone through various reactions (see Section 2.2), which cause the dried oil to have a completely different chemical composition. Even though absolute quantification is rarely used in the analysis of cultural heritage samples, relative quantification is very common. The first study to suggest the usage of fatty acid ratios was proposed by Mills in the 1960s. He demonstrated that the ratio of the two saturated fatty acid peak areas – palmitic acid to stearic acid (P/S ratio) – is characteristic of a specific oil and stays approximately the same during aging.[68] Since then, quite wide P/S value ranges have been reported for the most widespread drying oils – in rough terms, the P/S ratios are around 1.4–2.4 for linseed oil, 2–4.5 for walnut oil, and 3–8 for poppy oil.[69] Because these values have only a small overlap, the P/S ratio has been used as a differentiating parameter to suggest the type of the used oil.[70–74] The high variance in the P/S value of one type of oil is mainly caused by different oil pre-treatments and origins. However, several studies have suggested that the P/S ratio is not stable during the aging of a drying oil, but decreases in time.[21,32,75] During the drying processes, some of the TAGs are hydrolyzed, and free fatty acids are produced, including free palmitic and stearic acid.[75] A study by Schilling *et al.*[75] demonstrated that palmitic acid evaporates four times more rapidly than stearic acid, which would lead to the decrease of the P/S ratio.

Other common values derived from peak areas in chromatograms that are used to characterize drying oils are the ratio of azelaic acid to palmitic acid (A/P) and the sum of the relative content of dicarboxylic acids to other fatty acids (∑D). The higher these values, the more oxidized and therefore dried is the paint sample because dicarboxylic acids (including nonanedioic acid aka azelaic acid) are the autooxidation products of the unsaturated fatty acids.[32,64] It has been suggested that $A/P > 1$ together with $\sum D > 40\%$ are characteristic values of drying oils, and $A/P < 0.3$ together with $\sum D < 15\%$ are characteristic to egg (yolk, white, or whole egg) binder.[76,77]

Although in some cases the class or even the exact type of the binding material can be suggested based on these ratios, conclusions must be made

cautiously. Several studies have shown that various factors may influence the oil's drying processes (and through it also the P/S, A/P, and ∑D ratios) like the presence of other sample components (pigments,[34] fatty acids from waxes[69]) and storing conditions (UV exposure[78] and RH[31]). Additionally, some additives (for example, metal carboxylates – stearates and palmitates) that have a similar composition to the fatty acid residues affect the before-mentioned ratios.[21,79,80]

2.5. Uncertainty evaluation of derivatization

In this thesis, the quantitative analysis of oils was performed. Therefore, the uncertainty of the results must be evaluated. Based on the definition proposed by the International Vocabulary of Metrology (VIM), the measurement uncertainty is a "non-negative parameter characterizing the dispersion of the quantity values being attributed to a measurand, based on the information used".[81] This is a necessary parameter for the correct presentation of the results of a quantitative analysis which also characterizes the quality of the result.[82]

One aspect that directly influences the measurement uncertainty in the GC analysis of oils is the derivatization step. Derivatization is often one of the most complex steps in the GC and also LC analyses and, therefore, may have a large contribution to the uncertainty budget. For derivatization, a 100% derivatization efficiency (yield) is desired.[83] However, most of the time the derivatization efficiencies are below 100% – for example, the derivatization reaction may not proceed to completion, or there are analyte losses during transferring and/or solvent evaporations. Therefore, for the presentation of a correct quantitative result, the efficiency of the derivatization procedure and its uncertainty estimate should be included. However, the evaluation of the derivatization efficiency requires absolute quantification. In paper I, the derivatization efficiency and measurement uncertainty estimation were included as important factors for selecting the most suitable derivatization method. There the measurement uncertainty estimation was performed by calculating the intermediate precision (within-lab reproducibility) of the analysis – this is a top-down measurement uncertainty estimation value that is obtained by preparing and analyzing the sample on different days and calculating the standard deviation (standard uncertainty).[82]

Even though there are numerous studies that estimate the measurement uncertainty for GC and LC analysis involving derivatization (references 84–88, to name only a few), to the best of our knowledge, the uncertainty contribution of the derivatization step, specifically, has not been addressed. To evaluate the uncertainty contribution of only the derivatization step, a bottom-up uncertainty estimation approach can be applied. In bottom-up approaches, the uncertainties of all relevant input quantities are found and merged to yield a combined uncertainty of the output quantity.[89] Two well-known bottom-up approaches are the conventional GUM approach (termed as the law of propagation of uncertainty, described in the Guide to the Expression of Uncertainty in Measurement) and the Monte Carlo method (MCM).[82]

These two methods have been compared based on chemical analyses,[90–93] but in paper II, for the first time, the methods were compared in terms of the uncertainty of the derivatization step. Like almost all quantitative GC and LC analyses, the studied quantitative derivatization method involves linear regression. However, with linear regression, there are two ways to choose the input quantities (important uncertainty sources, see the following sections). Often, slope (a) and intercept (b) are chosen as the input quantities. The other option is to use the ratios of concentrations and signal intensities of the measured calibration solutions (that can be considered as the input quantities for a and b) as these are the primary values. When choosing the first option, the negative correlation between the slope and the intercept should be considered while estimating the uncertainty with the traditional GUM and MCM approaches. In the traditional GUM method, the correlation between input quantities can be taken into account. However, additional methods (Ilman-Conover,[94] Gaussian copula[95] – used in paper II) have to be included with the MCM to take the correlation between input quantities into account. In paper II, both ways – taking and not taking the correlation between input quantities into account – were considered with the traditional GUM and MCM methods. These approaches are discussed further in the following sections.

2.5.1. The traditional GUM method

In the traditional GUM approach,[96] first, the measurand is defined, a mathematical model is constructed, and the value of the measurand is calculated. Second, all important uncertainty sources are identified. Third, the uncertainties of the input quantities are calculated, and fourth, the combined (and often also the expanded, see below) uncertainty is calculated. In the uncertainty estimation of the measurand, the standard uncertainties of the input quantities are used to calculate the combined standard uncertainty of the output quantity. A functional relationship f connects the input quantities (x_1, x_2, ... x_n) to the output quantity (measurand Y) by equation (1):

$$Y = f(x_1, x_2, \ldots x_n) \tag{1}$$

The combined standard uncertainty – u_c – of the value Y can be calculated by combining the standard uncertainties of input quantities (x_i) by equation (2). The $\partial Y/\partial x_i$ is the sensitivity coefficient (partial derivative) and r(x_i, x_j) is the correlation coefficient of the two input quantities. The second term under the square root takes the correlation between quantities x_i and x_j into account – this can be disregarded from the formula if the input quantities are statistically independent.

$$u_c(Y) = \sqrt{\sum_i \left[\frac{\partial Y}{\partial x_i} \cdot u(x_i)\right]^2 + \sum_{i=1}^{n-1} \sum_{j=i+1}^{n} 2 \cdot r(x_i, x_j) \cdot \frac{\partial Y}{\partial x_i} \cdot \frac{\partial Y}{\partial x_j} \cdot u(x_i) \cdot u(x_j)} \quad (2)$$

After calculating the combined standard uncertainty, the expanded uncertainty can be obtained by multiplying the value by a suitable coverage factor. Often a coverage factor in the range of 2 to 3 is used, which results in a probability coverage level of roughly 95.5% to 99.7%. However, in the case of an input quantity whose uncertainty contribution is high (a strong influencer) and that is obtained via small number of replicate determinations, the distribution function is closer to the Student's distribution (aka *t*-distribution) than to the Normal distribution. Thus, the uncertainty distribution of the output quantity will be a convolution of the Normal and Student's distributions. Then, the distribution function of the output quantity is often assumed to have the Student's distribution with an effective number of degrees of freedom (v_{eff}). The Welch-Satterthwaite formula presented by equation (3) can be used to calculate the v_{eff}:

$$v_{eff} = \frac{{u_c}^4(Y)}{\sum_i \frac{\left[\frac{\partial Y}{\partial x_i} u(x_i)\right]^4}{v_i}} \quad (3)$$

In equation (3), the v_i represents the number of degrees of freedom for the input quantity x_i. After calculating v_{eff}, the expanded uncertainty of the output quantity at coverage probability P (often 95%) can be found by multiplying the combined standard uncertainty by the Student's coefficient $t(v_{eff}, P)$.

2.5.2. The Monte Carlo Method (MCM)

In the MCM,[97] instead of the standard uncertainties used in the traditional GUM approach, the propagation of actual distribution functions of the input quantities are used. This way, the MCM enables a more realistic evaluation of the uncertainty of the measurand without needing to calculate the partial derivatives.

In the MCM approach, random values from the probability density functions (PDF) of the input quantities are generated, and the corresponding value of the output quantity is found. This iteration is performed many times (typically 10^5–10^6 times). The values of the output quantity are combined, and its empirical distribution function is obtained. In Figure 5, the general scheme proposed by Herrador *et al.*[98] for the MCM simulation is presented. In the example, model Z depends on three input quantities (X_1, X_2, X_3) that have the corresponding PDF-s: $p(X_1)$ – rectangular, $p(X_2)$ – triangular, and $p(X_3)$ – normal. After performing the MCM simulations, a non-symmetric PDF is obtained for Z, $p(Z)$. From there, it is possible to calculate the mean and uncertainty of the output value.

The MCM is considered more universal than the traditional GUM method. For example, the MCM can manage input quantities with any distribution functions and cope with non-linearity caused by an input quantity. Additionally, the MCM simulation provides a better estimate of the real uncertainty coverage interval for the result.[99]

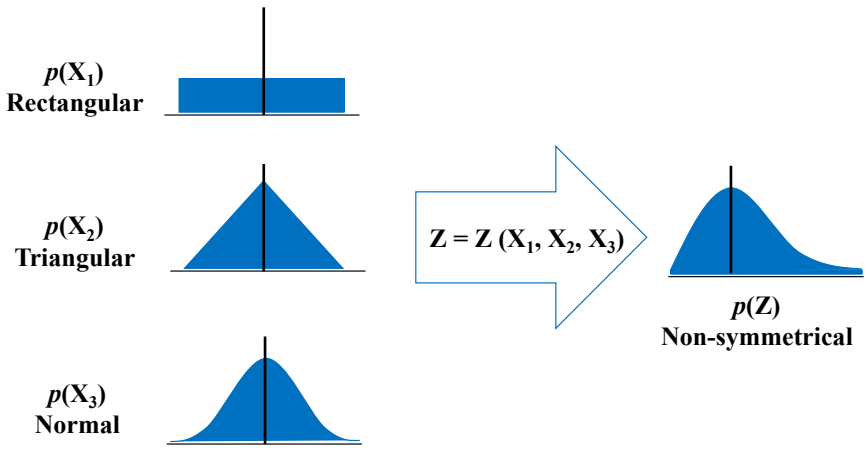

Figure 5. General scheme of the Monte Carlo Method (MCM).[98] The symbols are explained in the text above.

3. EXPERIMENTAL SECTION

The origin and purities of the chemicals and materials used in this thesis that are not presented here are given in paper I or paper III.

3.1. Quantitative analysis with GC-MS/FID

In the quantitative analysis, both the traditional relative quantification and the less used absolute quantification were performed. The relative quantification is a quicker method based on the peak area ratios of specific fatty acids or dicarboxylic acids. The absolute quantification also uses peak areas in the calculations and returns the absolute concentrations of the analytes as a result (expressed as grams or moles per 100 g of oil, for example), but the procedure is much more labor-intensive. The internal standard method was used for the absolute quantification. To visualize the calibration graphs, the analyte/internal standard peak area ratio (S_{AD}/S_{IS}) was plotted against the analyte/internal standard concentration ratio (C_{AD}/C_{IS}). For each derivative, a corresponding calibration graph was constructed (two representative calibration graphs are presented in Figure 6). Knowing the peak areas and concentration of internal standard, it is possible to calculate the concentration of the fatty acid derivative from the linear regression model, which can then be converted to represent the corresponding fraction of a TAG molecule.

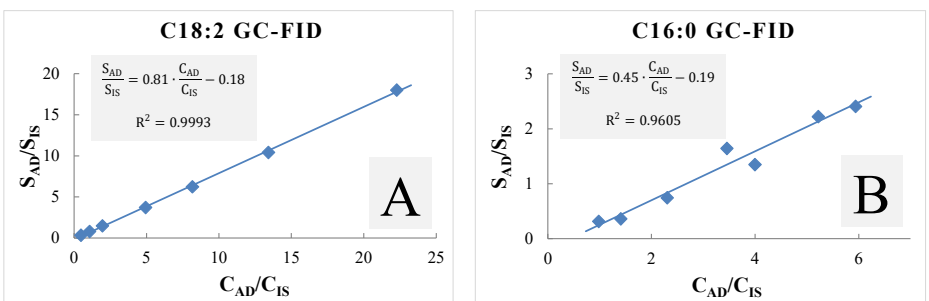

Figure 6. Representative calibration graphs of one of the best (A: methyl linoleate measured with GC-FID) and one of the worst (B: trimethylsilyl palmitate measured with GC-FID) examples.

Derivatives of the main fatty acids were used to make the calibration solutions. Three sets of standards were needed because different derivatives were produced with the used derivatization methods: TMTFTH and ACM methods give fatty acid methyl esters (FAME), NaOEt–BSTFA mainly fatty acid ethyl esters (FAEES), and KOH–BSTFA method yields fatty acid trimethylsilyl esters

(TMSE). The FAME and FAEES standard mixtures with known concentrations are commercially available and were used to prepare seven calibration solutions each. The FAME mixture (Sigma-Aldrich, St. Louis, MO, USA) contained methyl palmitate, methyl stearate, methyl oleate + methyl elaidate (*Z* + *E*), methyl linoleate, and methyl linolenate (papers I, III). In the quantitative analysis of yeast cells, another FAME mixture was used (C4–C24, Supelco, Bellefonte, PA, USA) because of availability. The FAEES mixture (Supelco) contained ethyl esters of saturated fatty acids, including ethyl palmitate and ethyl stearate (paper I). It was concluded that the analysis of these two ethylated fatty acids is sufficient for the characterization of the derivatization efficiency of the NaOEt–BSTFA procedure. Internal standard (IS, solution of hexadecane) was added to all calibration solutions. The calibration solutions and derivatized sample solutions were analyzed with GC-MS/FID in random order.

Because the TMSE standards of the studied fatty acids necessary for the KOH–BSTFA method were commercially unavailable, the TMSE of palmitic, stearic, and oleic acid were synthesized in-house. The synthesis was based on the protocol presented by Noda and Bode.[100] A Schlenk flask was heated overnight at 130 °C and thereafter cooled airtight in Ar flow. Depending on the desired TMSE, 0.25 g of palmitic, stearic, or oleic acid was placed into the flask. Anhydrous acetonitrile (0.7 mL) and BSTFA (0.7 mL) were added to the fatty acid, and the mixture was stirred for 3 h at 60 °C in Ar flow. Finally, the volatiles were removed from the flask during 3 h at 60 °C. The purities of the synthesized TMSEs were determined with the quantitative NMR method (qNMR).

For the comparison of the derivatization methods (paper I), two main validation parameters were used – derivatization efficiency (yield) and intermediate precision (within-lab reproducibility) – which together express the ruggedness of the method. Those values were calculated based on the analyses performed over several weeks, therefore, accounting also for random effects.[51,101] To evaluate those parameters, a mixture of TAGs (tripalmitin, tristearin, triolein, and trilinolein) was prepared by weighing to imitate the composition of natural oil. An analytical grade oil standard (canola oil, Supelco) was used as the quality control sample. Clarified linseed oil used for art (Lefranc & Bourgeois, Paris, France) and canola cooking oil (Olivia, Estonia) were used as real-life samples.

Intermediate precision was also calculated in paper III to assess the suitability of the chosen derivatization method for the analysis of dried oil paint mock-ups by analyzing one of the most homogenous samples (yellow ochre + linseed oil, 50 g/100 g) on five days among the GC-MS analysis of other oil paint mock-up sets.

3.2. Uncertainty estimation of the KOH–BSTFA derivatization

In paper II, the KOH–BSTFA method was chosen as an exemplary procedure to study the measurement uncertainty of the derivatization step. The data obtained from the analysis of the solution containing tripalmitin analyzed on one day was used in the mathematical model of derivatization efficiency. The GC-MS results of the calibration solutions measured on four days were averaged and used to construct the calibration graph corresponding to palmitic acid trimethylsilyl ester. The slope (*a*) and intercept (*b*) of this graph were used in the mathematical model.

Six uncertainty estimation methods based on the traditional GUM approach (marked as G) or the MCM (marked as M) were used. In the case of G1 and M1, the correlation between *a* and *b* was not taken into account. Conversely, in G2 and M2, the correlation between *a* and *b* was used (correlation coefficient r = -0.71). In the last two approaches, G3 and M3, instead of *a* and *b* as the input quantities, the uncertainties of the concentration ratios and signal ratios (used to construct the calibration graph) were used. This approach is called the "full" least-squares linear regression. GUM Workbench 2.3 software was used for the traditional GUM approach, and R software was used for the MCM and the Gaussian copula methods. In paper II, the comparison and analysis with the traditional GUM approach and MCM were performed by Dr. Martin Vilbaste.

3.3. Oil paint mock-ups

The seven analyzed oil paint mock-up sets contained a natural or synthetic pigment (zinc white, Prussian blue, yellow ochre, red ochre, natural cinnabar, chrome oxide green, or a mixture of hematite and kaolinite) and linseed oil. The paints had been prepared by weighing (Sartorius balance, resolution 0.1 mg) and mixing on Petri dishes. Each pigment and linseed oil mixture had 15 to 16 paint samples, where the oil concentration varied from 10 to 95 g/100 g. The paint samples had been artificially aged. The paint mock-ups containing Prussian blue, natural cinnabar, red ochre, chrome oxide green, or the hematite + kaolinite mixture had been aged in a specially made chamber with RH of 35 ± 10 % for six months at 72 ± 5 °C and then for four months at 62 ± 5 °C. The zinc white and yellow ochre paints were kept in a drying oven for eight months at 80 ± 2 °C. Then the paints were pulverized with a ball mill (Mini-mill Pulverisette 23, Fritsch), transferred into vials, and stored at room temperature away from direct sunlight. The GC-MS analysis and ATR-FT-IR measurements were performed after *ca.* nine months. Each pigment + linseed oil set was derivatized and analyzed with GC-MS in one series. Some pulverized paint samples (especially chrome oxide green and linseed oil samples) remained slightly inhomogeneous. Therefore, the pieces were carefully selected for the GC-MS analysis to get the averaged overview of the whole sample.

3.4. Derivatization procedures

The four derivatization procedures used in this thesis for the analysis of oils were based on literature and modified when needed to fit the requirements of the absolute quantification method. Analytical balances (GENIUS Sartorius or Precisa, both with a resolution of 0.01 mg) were used for weighing all the samples, solutions, and reagents that affected the concentration of the analyte(s) in the quantitative analysis. To perform an accurate and reliable absolute quantification, the minimum amount suitable for weighing with these balances is 10 mg. If there is a need for absolute quantification in smaller sample amounts (e.g., 1 mg), a balance with higher resolution (e.g., 0.001 mg) should be used. However, if relative quantification is sufficient then highly accurate weighing is not important. In paper I, stock solutions of samples (fresh oils and TAG standards) were made in toluene and smaller volumes were measured from them. This way, the sample amounts used in the derivatization would be similar to those used in the literature. In paper I, the details of the four derivatization methods are presented. In paper II, the KOH–BSTFA method was studied in terms of uncertainty estimation. In paper III, the ACM procedure was used and explained further. Hexadecane was used as the internal standard (IS). In this thesis, another derivatization method developed for the analysis of proteins (HCl–MTBSTFA method: hydrolysis with HCl, followed by derivatization with methyltributylsilyl tetrafluoroacetamine) was used only for the analysis of the case study paint samples (see Section 4.5.1).

TMTFTH derivatization

The TMTFTH derivatization was based on the procedure presented by Manzano *et al.*[102] TMTFTH solution in methanol (50 µL) was added to the stock solution in a glass vial. The derivatization mixture was sonicated for 30 min. Then, the solution was left to stand for 24 h at room temperature as suggested by Sutherland[60] because it became evident that with the samples analyzed in paper I, the time span used in the original work[102] was not sufficient for complete derivatization. Finally, the solution was diluted in DCM and IS was added.

NaOEt–BSTFA

The two-step derivatization with NaOEt and BSTFA was based on the procedure presented by van den Berg *et al.*[65] NaOEt 0.01 M solution in ethanol was added to the stock solution. Dry nitrogen was purged through, the vial was crimped with a cap and heated for 1.5 h at 70 °C. Then, NH_4Cl saturated solution in ethanol was added to the mixture. After 20 min, the solvents were evaporated, the residue redissolved, and BSTFA added. Again, the vial was crimped with a cap and heated for 30 min at 70 °C. The solution was quantitatively transferred to another vial and evaporated to dryness. The analytes were redissolved in DCM and the IS stock solution was added.

KOH–BSTFA

The second two-step derivatization with KOH and BSTFA studied in papers I and II was based on the method described by Lluveras *et al.*[103] First, the stock solution was evaporated to dryness, and 10 wt% KOH solution in ethanol was added to saponify the TAGs. The vial was crimped with a cap and heated for 2 h at 60 °C. Then, Milli-Q water and TFA solution were added to produce free fatty acids. The solution was extracted with hexane and diethyl ether. The combined extracts were evaporated to dryness, isooctane and BSTFA were added. The mixture was heated for 30 min at 60 °C. Then, the solvents were evaporated, the residue redissolved in isooctane, and the IS stock solution was added.

ACM

The ACM was based on the method described by Craig *et al.*[104] Compared to their work[104] and paper I, the heating parameters were changed in paper III because it was found that shorter heating at higher temperature was also suitable. In paper I, the stock solution was evaporated to dryness. In paper III, 10 to 12 mg of pulverized oil paint mock-up sample was weighed. In both papers, methanol was added to the dry sample, and the vial was sonicated for 15 min. Then, concentrated H_2SO_4 was carefully added to the methanolic solution, the vial sealed with a PTFE-lined screw cap, and heated (4 h at 70 °C in paper I, 3 h at 80 °C in paper III). After the reaction mixture had cooled to room temperature, the solution was extracted three times with hexane. The hexane layer was carefully separated and pipetted into another vial through a glass pipet filled with a layer of K_2CO_3 upon a layer of glass wool. The combined extracts were evaporated to dryness. The residue was redissolved in hexane or toluene and IS stock solution added. The same procedure that was used for the analysis of oil paint mock-up samples was used for the analysis of yeast cells.

For the case study paint samples (see Section 4.5.1), around 0.1–0.3 mg of paint was transferred to a 15 mL vial. Then, 1 mL of methanol was added, the vial was sonicated for 15 min, and 0.2 mL of concentrated H_2SO_4 was carefully added. The sample, solvents, and reagents were not accurately weighed because only relative quantification was performed with these samples. The other aspects of the sample preparation were the same as in paper III, described in the previous section. To the residue obtained from the extraction, 0.1 mL of toluene was added, and this solution was analyzed with the GC-MS (without IS).

HCl–MTBSTFA (for amino acid analysis)

The amino acid derivatization was based on the procedures described by Pitthard *et al.*[105] and Lluveras *et al.*[103] A simplified procedure was used because the aim was to determine if the case study paint samples from the cultural heritage objects contained proteins, not to quantify the amino acids. Around 0.1 mg of sample was transferred into a chromatographic vial and 100 µL of 6M HCl (prepared from concentrated HCl, >37%, Sigma Aldrich, and Milli-Q water). The vial was purged through with N_2, crimped with a cap, and heated

for 24 h at 105 °C. After the vial had cooled to room temperature, the sample was evaporated to dryness at 60 °C under N_2 flow. Then, 40 µL of Milli-Q water was added to the residue, the solution stirred, and evaporated to dryness. The same procedure was performed with 40 µL ethanol (Estonian Spirit OÜ, Estonia purity 96.7%). To the residue, 20 µL of MTBSTFA (Sigma-Aldrich, purity >97%), 20 µL of pyridine (Honeywell, Charlotte, NC, USA, purity >99.8%), and 2 µL of triethylamine (Sigma-Aldrich, purity ≥99%) were added. Again, the vial was crimped with a cap and the derivatization mixture was heated for 30 min at 60 °C. After the solution had cooled to room temperature, 20 µL of the solution was transferred to a chromatographic vial with a 100 µL insert and centrifuged. From the supernatant, 10 µL was transferred to another chromatographic vial with a 100 µL insert and analyzed with GC-MS.

3.5. Parameters of the used instruments

GC-MS/FID

For the lipid analysis with GC, the following Agilent devices were used: 7890A GC connected to 5975C inert XL MSD with a Triple-Axis Detector and a G4513A autosampler. The column was an Agilent DB–225MS capillary column (50% cyanopropylphenyl-50% methylpolysiloxane) with dimensions of 30 m x 0.25 mm and a film thickness of 0.25 µm. The temperature of the ion source was 230 °C, the mass spectrometer transfer line 280 °C, and the inlet 300 °C. The injection volume was 1 µL (papers I and II), 0.5 µL (paper III and analysis of yeast cells), or 2 µL (analysis of the paint case study samples). Electron impact ionization (EI) with 70 eV electrons was used, and the solvent delay was 5 min (papers I and II) or 5.60 min (paper III, yeast cells, and paint case study samples). The splitless mode was used with the split opened after 2 min. The carrier gas was helium 6.0 with a flow rate of 1.5 mL/min. The temperature in FID was 300 °C. The H_2 and airflow rates were 30 and 400 mL/min, respectively.

The temperature programs were the following: initial temperature 80 °C, isothermal hold for 2 min, temperature ramp of 10 °C/min (papers I and II) or 20 °C/min (paper III, yeast cells, and paint case study samples) to 200 °C, and 4 min hold. Then, the temperature was increased again at 5 °C/min to 220 °C, isothermal hold for 5 min, and in the end 10 °C/min to 230 °C (isothermal hold in paper III, for the yeast cells and paint case study samples for 12 min). The total run time in papers I and II was 28 min, and in paper III, for yeast cells, and for paint case study samples, 34 min. These temperature programs enabled the efficient separation of all fatty acids and their degradation products, except for the two isomers of octadecenoic acid, C18:1 (oleic and elaidic acid). In the case of this thesis, it is acceptable to present the sum of these isomers as is usually done to characterize the content of C18:1 in oils.[2,4,20]

In papers I and II, the MS was operated in the scan mode, where the total ion chromatogram (TIC) was recorded in the mass range of 50–800 *m/z*. In

paper III, for the yeast cells, and the case study paint samples, the qualitative analysis was performed in the scan mode (mass range 27–400 *m/z*) and the quantitative analysis in the SIM (selected ion monitoring) mode. In SIM mode, at the start of the run, the ions with *m/z* values of 57 and 71 were measured to register the IS. After 9.5 min, the signals corresponding to ions with *m/z* values of 55, 74, and 81 were registered. These ions correspond to one of the most intense fragments present in the mass spectra of methylated fatty acids. For the data analysis, an Agilent MSD ChemStation and NIST Mass Spectral Library Search 2.0 were used.

For the amino acid analysis (used only for the analysis of the case study paint samples from the cultural heritage objects), another GC-MS system consisting of Agilent devices was used: 6890N GC connected to a 5973 MS and a G2613A autosampler. An Agilent DB–5MS capillary column was used (5% phenyl-95% methylpolysiloxane) with dimensions of 30 m x 0.25 mm and a film thickness of 0.25 μm. The temperature of the ion source was 230 °C, the mass spectrometer transfer line 250 °C, and the inlet 220 °C. The injection volume was 1 μL. Electron impact ionization (EI) with 70 eV electrons was used, and the solvent delay was 5.20 min. The split mode with a split ratio of 2:1 was used (split flow 2.3 mL/min). The carrier gas was helium 6.0 with a flow rate of 1.1 mL/min. The temperature program was the following: initial temperature 100 °C, isothermal hold for 2 min, temperature ramp of 4 °C/min to 280 °C, and 15 min hold with a total run time of 62 min. The MS was operated in the scan mode (mass range of 20–400 *m/z*).

NMR

For the ^{1}H NMR measurements, Bruker Avance 700 spectrometer working at 700.1 MHz was used. The spectra were recorded at 25 °C in $CDCl_3$ (99.8% D + 0.03% TMS). The synthesis yields and purities of the TMSE were the following: palmitic acid TMSE (yield 79%; purity 99.1%), stearic acid TMSE (yield 47%; purity 95.4%), and oleic acid TMSE (yield 37%; purity 99.2%).

ATR-FT-IR

A Thermo Scientific Nicolet 6700 FT-IR spectrometer with Smart Orbit diamond micro-ATR accessory (refractive index – 2.4, the diameter of the active sample area – 1.5 mm) was used for the ATR-FT-IR analysis. The FT-IR spectrometer was equipped with a DLaTGS detector, Vectra Aluminium Interferometer, and a CsI beamsplitter. For recording ATR-FT-IR spectra, the wavenumber range of 4000–225 cm^{-1}, resolution 4 cm^{-1}, and the number of scans 128 were used. Constant dry air purging was used to protect the FT-IR spectrometer from atmospheric moisture. Thermo Electron's OMNIC 9 software was used to collect and process the spectra.

4. RESULTS AND DISCUSSION

4.1. Quantitative GC-MS/FID analysis with the derivatization methods

The modified quantitative analysis with the four derivatization methods (TMTFTH, NaOEt–BSTFA, KOH–BSTFA, and ACM) was performed on fresh oils and a self-made TAG mixture. The aim was to compare the four derivatization methods and to describe each one's advantages and disadvantages. In the following sections, the results of both relative and absolute quantification of TAGs with the improved methods are presented. The results include the comparison based on sample preparation, intermediate precision, and derivatization efficiency of each derivatization method.

4.1.1. Relative quantification of the canola oil standard

For the initial evaluation of the four derivatization methods, an analytical grade canola oil standard was analyzed (Table 1 in paper I). The peak areas of the derivatized fatty acids were used to calculate the relative peak area percentages. These values were compared to the percentages presented in the canola oil certificate. The results showed that the derivatized fatty acids were efficiently separated by the used GC method and that all chosen derivatization procedures produced comparable and reproducible results in terms of the relative quantification of fatty acids.

4.1.2. Derivatization efficiency (yield)

To assess the derivatization efficiency (yield) of the derivatization procedures, absolute quantification is needed. For this aim, the self-made TAG mixture with known concentrations was analyzed with the improved absolute quantification method (see Section 3.1). In theory, if the concentrations obtained from the experiments would be the same as the concentrations calculated from the weighing data, then the derivatization efficiency would be 100%, meaning that all the TAG molecules were quantified. In Table 2, only the results of the GC-MS analysis are demonstrated because similar results were obtained with both MS and FID as detectors. Therefore, it can be concluded that both detectors would be suitable for the GC analysis of fresh vegetable oils. The GC-FID results are presented in paper I.

Table 2. Derivatization efficiency (%) based on the GC-MS analysis[a]

Sample	Fatty acid	TMTFTH GC-MS	NaOEt–BSTFA GC-MS	KOH–BSTFA GC-MS	ACM GC-MS
TAGs mixture	**C16:0**	102.3 (1.4)	67.3 (1.5)	97.0 (6.0)	96.8 (3.2)
	C18:0	93.7 (2.7)	60.3 (2.3)	87.9 (7.8)	74.2 (3.1)
	C18:1	98.3 (2.3)	–	100.3 (7.8)	85.5 (3.0)
	C18:2	90.1 (1.3)	–	–	77.4 (0.7)

[a] Every result is the average of three or four values determined over at least four weeks. In parentheses are the standard deviations. Some values could not be calculated (marked as "–") because the corresponding calibration solutions did not contain these fatty acid derivatives.

The results in Table 2 show that the TMTFTH derivatization had the highest derivatization efficiencies together with one of the best within-lab reproducibilities. The second-best in terms of derivatization efficiency would be the KOH–BSTFA method. However, for this method, higher standard deviations were seen. The ACM procedure had lower derivatization efficiencies than the above-mentioned methods, but better within-lab reproducibility than the KOH–BSTFA method. The method with the most unsatisfactory results was the NaOEt–BSTFA derivatization. The reason could be that NaOEt is not sufficiently strong to transesterify the TAG molecules in quantitative terms.

Therefore, although the relative quantification of the canola oil standard showed similar results for all four derivatization methods, the absolute quantification demonstrated that the methods are not equal in terms of derivatization efficiency. Additionally, from Table 2, it can be inferred that the derivatization efficiency of a derivatization method also depends on the specific fatty acid. Therefore, the used derivatization method is another factor that contributes to the wide variance of the P/S ratio obtained for one type of oil. For example, in case of an oil containing equivalent amounts of palmitic (C16:0) and stearic (C18:0) acid, the P/S ratio obtained with the TMTFTH method would be around 1.09; however, with the ACM derivatization the P/S value would be much higher – around 1.30.

4.1.3. Absolute quantification of fresh oils

The developed absolute quantification method was applied for the analysis of fresh clarified linseed oil, canola cooking oil, and the canola oil standard (all results are presented in Table 3 of paper I). In Figure 7, a representative chromatogram of the derivatized clarified linseed oil is presented.

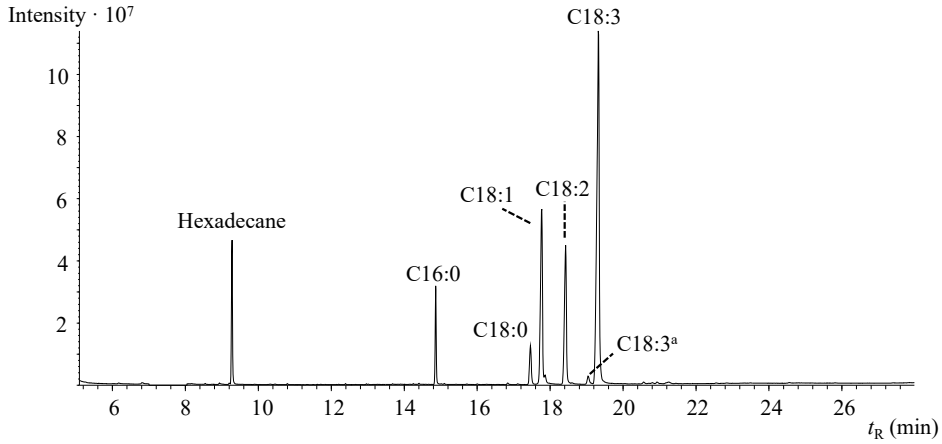

Figure 7. Representative TIC of the solution containing internal standard and TMTFTH derivatized clarified linseed oil. [a] Geometric isomer of C18:3.

In the case of the canola oil standard, it was possible to compare the obtained values to the ones presented in the certificate (Table 3) after converting the values into mmol/100 g units. The TMTFTH derivatization showed its superiority again by producing the highest fatty acid contents for the analyzed oils. The values obtained with the TMTFTH derivatization for the canola oil standard were also the closest to the certificate values. For the absolute quantification of oils, the second best was the ACM method (compared to the third position in the TAG mixture analysis).

Table 3. Absolute quantification of fatty acids in canola oil standard (mmol/100 g of oil) based on the GC-MS analysis.[a]

Sample	Fatty acid	TMTFTH GC-MS	NaOEt–BSTFA GC-MS	KOH–BSTFA GC-MS	ACM GC-MS	Certificate
Canola oil standard	**C16:0**	15.6 (0.1)	8.6 (0.6)	11.4 (1.8)	14.4 (1.2)	16.0
	C18:0	6.8 (0.2)	4.3 (0.5)	9.3 (5.0)	6.4 (0.6)	6.3
	C18:1	203.4 (2.6)	–	123.8 (19.4)	175.5 (19.3)	205.4
	C18:2	59.8 (0.3)	–	–	51.2 (4.9)	69.1
	C18:3	22.0 (0.2)	–	–	18.6 (1.3)	29.6

[a] Every result is the average of three values determined over at least four weeks. In parentheses are the standard deviations. Some values could not be calculated (marked as "–") because the corresponding calibration solutions did not contain these fatty acid derivatives.

Although the TMTFTH derivatization performed the best in terms of derivatization efficiency and within-lab reproducibility, it can be seen from Table 3 that the concentrations of C18:2 and C18:3 do not agree so well with the

certificate values as do the concentrations of C16:0, C18:0, and C18:1. For example, the derivatization efficiency with the TMTFTH method for C18:2 was 90.1% (see Table 2). When taking this derivatization efficiency into account, the concentration of C18:2 in the canola oil standard would be 65.9 mmol/100 g of oil, which agrees much better with the certificate value. This demonstrates that even when using the best derivatization procedures, the derivatization yield should be considered when presenting the absolute quantities.

In the case of clarified linseed oil and canola cooking oil, also the relative amounts of the quantified fatty acids were found with the TMTFTH and ACM derivatization methods (with these methods, the absolute quantification of all five main fatty acids was possible because the FAME mixture contained all corresponding derivatives). The results of these two methods agreed with the literature values reported for linseed and canola oil (see Table 4 in paper I). This again suggests that even when a derivatization method shows to be suitable for relative quantification, the usage of absolute quantification must be validated in terms of derivatization efficiency.

4.2. Concise comparison of the four derivatization methods

In addition to evaluating derivatization efficiency and intermediate precision, the experimental aspects of the four derivatization methods were compared (a concise comparison is presented in Table 4). Here again, the TMTFTH derivatization showed the highest number of advantages – the technique has readily available calibration standards, easily interpretable chromatograms, and the sample preparation was the quickest and the least labor-intensive. However, the cost of the chemicals was the highest. The other studied methods may be preferred, for example, if low-cost chemicals are needed, the aim is to distinguish between free and bound fatty acids, or the usage of readily available chemicals is needed. Although, it should then be considered if the aim is the relative or absolute quantification and if and how the derivatization efficiency should be taken into account.

Additionally, it must be kept in mind that the performed comparison is based on the absolute quantification of fresh oils. If the nature of the sample is different (e.g., dried and aged oil) or significant modifications are made to the procedures, then a re-examination of the order of these derivatization methods is necessary. For example, in the case of dried oils, stock solutions cannot be made because the polymerized structure does not fully dissolve in common solvents or solvent mixtures, and the method should be modified accordingly. Therefore, the conclusions derived from the analysis of fresh oils cannot be directly transferred for the study of dried oils. In paper I, the comparison was based on fresh oils because for finding the derivatization efficiencies, the exact composition of the sample (e.g., the TAG mixture) must be known. However, making an aged oil sample with known fatty acid concentrations is practically impossible.

Table 4. Comparison of the derivatization methods for fresh oils studied in paper I (green – advantages, red – limitations, black – neutral features).

	TMTFTH	NaOEt–BSTFA	KOH–BSTFA	ACM
Sample preparation	· One-step derivatization · No sample transfer necessary · Easy procedure	· Two-step derivatization · Evaporation · Labor-intensive	· Two-step derivatization · Evaporation · Labor-intensive	· One-step derivatization · Extractions · Evaporation · Labor-intensive
Type of derivatives	· Methyl esters	· Mainly ethyl esters	· Trimethylsilyl esters	· Methyl esters
Time required for sample preparation [a]	1 h	4 h	4 h	7 h
Approx. cost of chemicals for 100 derivatizations	145 €	65 €	70 €	60 €
Interpretation of results	Simple interpretation – one peak for every fatty acid	Possible to distinguish between free and bound fatty acids; interpretation is complicated by two peaks for every fatty acid	Interpretation may be complicated if several derivatives appear	Simple interpretation – one peak for every fatty acid
Average derivatization efficiency (SD) [b]	96 (2) %	64 (2) %	95 (7) %	83 (3) %

[a] The times do not include the time required for the synthesis of TMSEs, the NMR analysis for the quantitative analysis (KOH–BSTFA method), or the preparation of calibration solutions (all derivatization methods). [b] The average derivatization efficiency value was calculated by averaging the results obtained with one derivatization method using GC-MS or GC-FID. SD is the pooled standard deviation.

4.3. Uncertainty estimation with the traditional GUM and MCM

The previous sections demonstrated that within-lab reproducibility is one of the important factors when choosing a suitable derivatization method. Therefore, it is reasonable to put effort into evaluating (and reducing, if it is possible) the uncertainty of the derivatization step in the GC-MS analysis during the method validation. Next, the aspects and results of the two uncertainty estimation approaches (traditional GUM and MCM) applied for the KOH–BSTFA derivatization method are presented.

Even though the previous section showed that the TMTFTH derivatization is the preferred method for the absolute quantification of fresh oils, for the

uncertainty estimation, the KOH–BSTFA method was chosen for two reasons. First, the KOH–BSTFA method is a two-step derivatization and more laborious (including extraction, heating, and evaporation to dryness) than the TMTFTH derivatization. Therefore, the KOH–BSTFA is more suitable to model a typical GC or LC derivatization, which often involves multiple operations during sample preparation. Second, the calibration curves obtained from the analysis of the TMSE standards had the highest scatter (see a representative calibration curve in Figure 6B), which leads to a higher uncertainty contribution of the slope and intercept. This, in turn, could help to observe the impact of taking (or not taking) the correlation between the slope and intercept into account when estimating measurement uncertainty.

4.3.1. The contributions of input quantities

Both uncertainty estimation approaches (traditional GUM and MCM) require a measurement model that relates the input quantities to the output quantity. Therefore, the following measurement model was composed for the derivatization efficiency calculation (the mathematical model showing also the canceled-out components is presented in paper II):

$$R = \left(\frac{Y-a}{b \cdot pur}\right) \cdot \left(\frac{\Delta m_3 \cdot m_{\mathrm{IS}}}{m_{\mathrm{solvent3}}}\right) \cdot \left(\frac{m_{\mathrm{solvent1}} + m_{\mathrm{tripalm}}}{\Delta m_1 \cdot m_{\mathrm{tripalm}}}\right) \cdot \left(\frac{M_1}{M_2}\right) \quad (4)$$

The abbreviations in equation (4) denote the following values: R – derivatization efficiency, Y – the ratio of the peak areas (S_{AD}/S_{IS}), a – slope, b – intercept, pur – purity of the palmitic acid trimethylsilyl ester, Δm_3 – the mass of the IS solution weighed for the analysis, m_{IS} – the mass of IS used for preparing the IS stock solution, $m_{solvent3}$ – the mass of solvent used for preparing the IS stock solution, $m_{solvent1}$ – the mass of solvent used for preparing the tripalmitin stock solution, $m_{tripalm}$ – the mass of tripalmitin used for preparing the tripalmitin stock solution, Δm_1 – the mass of the tripalmitin solution weighed for the analysis, M_1 – the molar mass corresponding to one-third of tripalmitin, and M_2 – the molar mass of palmitic acid trimethylsilyl ester.

In Table 5, the units, values, uncertainties, and PDFs of the previously described input quantities are shown. The values of these input quantities are obtained from weighing, measuring the calibration solutions with GC-MS, or determining the purity (of palmitic acid trimethylsilyl ester) with NMR. The standard uncertainties of these values were found as follows. Uncertainties *u(a)* and *u(b)* were assumed to be equal to the standard deviations of the respective coefficients and calculated with the MS Excel LINEST function. All *u(m)* were evaluated based on the technical parameters of the balance (instability of readings, calibration, resolution, and linearity). Uncertainty due to non-ideal purity of the standard substance *u(pur)* was estimated from an assumed rectangular distribution with a mean value of 0.99 and maximum of 1.00, and

u(Y) from the standard uncertainty of the mean of peak area ratios but taking the correlation between *Y* and C_{AD}/C_{IS} into account.

Table 5. Information about the input quantities.

Quantity	Unit	Value	Standard uncertainty	PDF
Y	1	2.35	0.04	Student's (ν = 3)
a	1	-0.383	0.091	Normal
b	1	0.752	0.024	Normal
pur	1	0.99	0.0058	Rectangular
Δm_3	g	0.06640	0.00018	Normal
m_{IS}	g	0.01384	0.00015	Normal
$m_{solvent3}$	g	31.75727	0.00045	Normal
$m_{solvent1}$	g	23.82459	0.00045	Normal
$m_{tripalm}$	g	0.01036	0.00015	Normal
Δm_1	g	0.21332	0.00021	Normal

In Figure 8, the contributions of the input quantities to the uncertainty of the output quantity (derivatization efficiency) are presented for the G1 and G2 approaches. Through the pie chart, remarkable differences in the contribution are demonstrated when the correlation between the slope (*a*) and the intercept (*b*) is taken into account (G2) and when it is not (G1). In the case of the G1 approach, the uncertainties of the *a* and *b* are responsible for 78% of the entire uncertainty budget. However, in the G2 approach, the joint uncertainty of these two inputs is noticeably lower, 51%. The uncertainties of the other input quantities stayed the same, meaning that the remarkable difference comes only from the fact that the correlation between *a* and *b* was taken into account. The next largest contributors are the uncertainties of the ratio of the peak areas (*Y*), the mass of internal standard (m_{IS}), and the mass of tripalmitin ($m_{tripalm}$). The masses of the last two input values were the lowest, due to which a higher relative uncertainty was obtained.

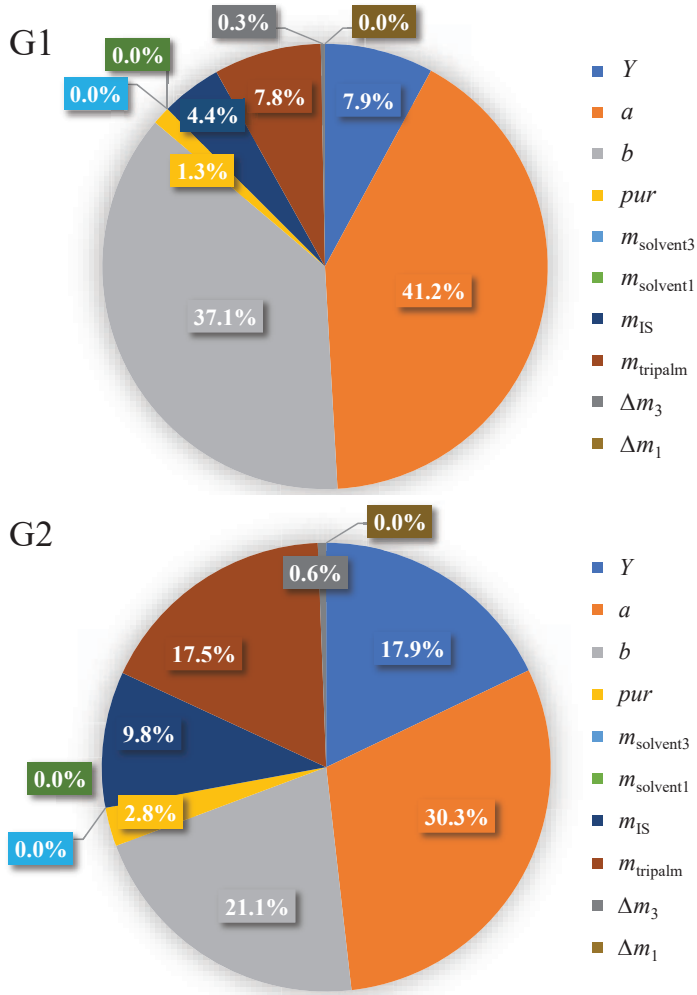

Figure 8. The contributions of the input quantities to the uncertainty of the output quantity (derivatization efficiency) in the case of the G1 approach (without taking the correlation between a and b into account) and the G2 approach (accounting for the correlation).

Therefore, for a lower uncertainty, it is reasonable to put effort into lowering the uncertainties of *a* and *b*. Besides taking the correlation between these input values into account, other measures can be taken. For example, it is beneficial to choose a derivatization method, where the standards for the calibration graph are stable and readily available. Additionally, measuring a larger number of calibration solutions can lower the uncertainties of *a* and *b*. Here it was also seen that weighing higher amounts of analytes/solvents reduces their relative uncertainty and, therefore, also the overall combined uncertainty.

4.3.2. Comparison of the traditional GUM and MCM approaches

All six procedures applying the traditional GUM and MCM approaches (G1, G2, G3, M1, M2, and M3 described in Section 3.2) were used for the uncertainty estimation of the KOH–BSTFA derivatization in the GC-MS analysis of a solution containing a TAG (tripalmitin). The results are presented in Table 6, where R represents the output value (derivatization efficiency), $u_c(R)$ is its combined standard uncertainty, and k is the coverage factor.

Table 6. Results of the six measurement uncertainty calculation approaches.

Approach	R^a	$u_c(R)$	Coverage interval, $P = 95.45\%$	Average expanded uncertainty	k	Assessment of uncertainty
G1	0.939	0.0488	(0.841…1.037)	0.098	2.00	Overestimated
M1	0.940	0.0525	(0.839…1.048)	0.105	–	Overestimated
G2	0.939	0.0325	(0.874…1.004)	0.065	2.00	Somewhat underestimated
M2	0.939	0.0379	(0.867…1.014)	0.074	–	Realistic
G3	0.939	0.0333	(0.872…1.006)	0.067	2.00	Somewhat underestimated
M3	0.940	0.0385	(0.866…1.017)	0.076	–	Realistic

[a] In the traditional GUM approaches (G1, G2, G3), the value is an individual value obtained from one experiment. In the MCM approaches (M1, M2, M3), this is the average value obtained from the simulation.

In Figure 8, the comparison of the uncertainty contributors in the case of G1 and G2 demonstrated that the correlation between the slope and intercept needs to be taken into account. Table 6 shows that neglecting the correlation leads to a (42–50)% overestimation of the expanded uncertainty. By comparing the results of the G2 and M2 methods to the respective results of the approaches containing the "full" linear least-squares regression method (G3 and M3), it can be seen that similar values were obtained. The G3 and M3 automatically take the correlation between the slope and the intercept into account because these approaches contain the uncertainties of the concentration ratios and signal ratios as input quantities instead of slope and intercept. These similar results suggests that both approaches can be used to find the combined uncertainty of the output quantity (if the correlations between input quantities are taken into account). Comparing the traditional GUM and MCM approaches to one another, it can be seen that slightly higher (1.07–1.12 times) average expanded uncertainty values were obtained for the MCM approach. The main contributor of the slightly lower values in the case of the traditional GUM approach is the uncertainty of the ratio of peak areas $u(Y)$, which is probably underestimated because of the low Student's coefficient provided by the Welch-Satterthwaite formula (equation 3). As shown in Figure 8, the uncertainty of the ratio of peak areas $u(Y)$ was

also one of the most significant uncertainty contributors. Therefore, the MCM can be considered the preferred approach as the M2 (combined, for example, with the Gaussian copula method to enable taking correlations between input quantities into account) or the M3 method. Comparing the M2 and M3 approaches to one another, the advantage of the M2 approach is the fact that the number of input quantities is lower than for the M3 approach (containing all concentration ratios and signal ratios). However, the M3 approach may be preferred because then the need for an additional method (Gaussian copula or Ilman-Conover) for taking the correlation between input quantities into account can be avoided.

The frequency distributions for the derivatization efficiency (output quantity) in the case of M2 and G2 (having a Student's PDF) are presented in Figure 9. As can be seen, the MCM frequency distribution is slightly tilted to the right, meaning it is nonsymmetric. The non-symmetric distribution is caused by input uncertainties that in the measurement model have nonlinear behavior, such as inputs that are in the denominator.[106] In our case, one input in the denominator is the intercept (*b*) that also has one of the highest uncertainty contributions to the derivatization efficiency (Figure 8) and therefore contributes the most to the nonsymmetric distribution. This comparison demonstrates that the MCM approach is able to take the small nonlinear effect caused by this input value to the derivatization efficiency into account.

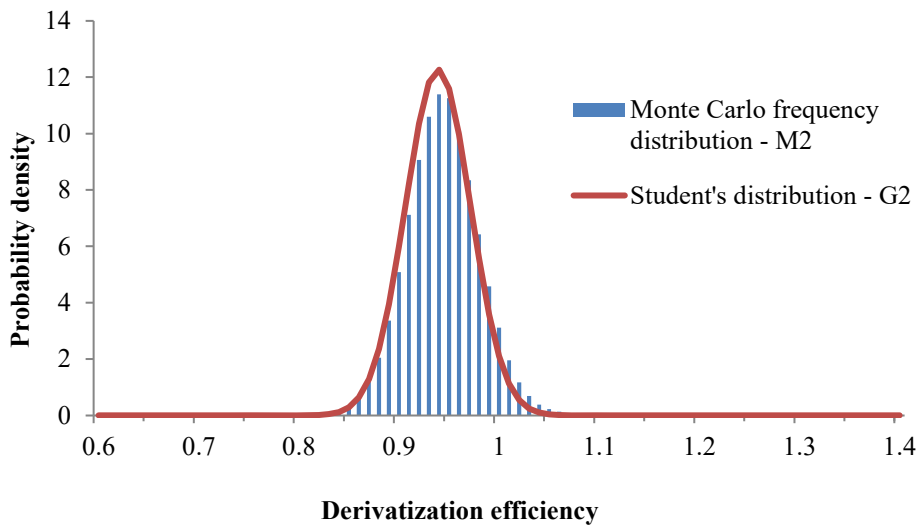

Figure 9. Frequency distributions of derivatization efficiency in the case of M2 and G2 approaches.

4.3.3. Intermediate precision vs. traditional GUM and MCM

When comparing the derivatization efficiency of tripalmitate with KOH–BSTFA method presented in paper I (R = 0.97, Table 2) to the results presented in Table 6 (average value of R = 0.94), it can be seen that the values differ. The reason is that in paper I, the derivatization efficiency was obtained as the average values of four independent quantitative analyses (in the range of 0.89–1.04). In paper II, the results obtained via the traditional GUM approach were the individual values obtained from one analysis, and the MCM derivatization efficiencies were the average values obtained from the simulation. Therefore, these values do not have to match. When observing the uncertainty values in paper I, the intermediate precision was calculated as the standard deviation of the four measurement results (0.060). This intermediate precision as uncertainty estimation characterizes the overall performance of the analytical procedure and should take most of the uncertainty sources into account, except for those that do not reveal themselves even if the individual experiments have been performed over a sufficiently wide time range (named lab/method bias). The standard deviation of the mean of the four measurements is then 0.030. In the case of M2 and M3, the combined standard uncertainties were a little bit higher – 0.038. From these values it is possible to calculate the method bias based on equation (5)[107]:

$$u_c = \sqrt{u(R_w)^2 + u(bias)^2} \quad (5)$$

In equation (5), the u_c represents the combined standard uncertainty (0.038), the $u(R_w)$ represents the uncertainty due to random effects (0.030), and the $u(bias)$ is the uncertainty due to method bias. In this case, the bias corresponds to standard uncertainty around 0.023, which suggests that the main contributors to the uncertainty of derivatization efficiency are the long-term effects and that the bias is a lower contributor.

4.4. Analysis of the oil paint mock-ups

The developed absolute quantification method and a suitable derivatization method were used for the analysis of artificially aged pigment and linseed oil mixtures (paper III). Dried linseed oil has mainly polymeric structure, the content of unsaturated fatty acids has decreased (only the less reactive oleic acid may be found to some extent), and degradation products (mainly dicarboxylic acids) have formed. Because of the polymeric structure, the dried oil does not fully dissolve in the commonly used solvents. Therefore, additional factors need to be considered when choosing a suitable sample preparation procedure.

For the analysis of dried paint mock-ups in paper III, ACM derivatization was chosen because of the large sample amount (at least 10 mg) and the high number of samples (110). As shown in Table 4, ACM is the least expensive

derivatization method compared to the other methods studied in paper I, which is advantageous in the case of a high number of large samples. Additionally, the method yields methylated fatty acids. Therefore, the commercially available FAME mixture can be used to make the calibration solutions (which enables the quantification of oleic acid that is absent from the FAEES mixture needed for the NaOEt–BSTFA derivatization). Also, the preferred method used for the absolute quantification of fresh oils in paper I – the TMTFTH derivatization – was tested. However, it became evident in paper III that the used TMTFTH procedure is not efficient enough for the absolute quantification of fatty acids present in dried and polymerized paint samples. In case of this procedure, one reason could be the high sample amount (10 mg) needed for accurate weighing with an analytical balance (resolution of 0.01 mg) and for obtaining a better overview of the whole sample. After 24 h, it was visually possible to see that the dried oil had not fully dissolved in the derivatization mixture. Therefore, heating for 1 h at 60 °C was tested (as was done by Pitthard *et al.*[70]). However, this did not significantly improve the derivatization and still most of the sample remained undissolved. Additionally, 0.5 mL of reagent (usually much lower volumes, 15–50 μL[70,102,paper I] are used) was tested, but even such a high reagent volume was not sufficient enough to produce such a high amount of derivatized analytes as did the ACM procedure.

The chromatographic profile of the methylated fatty acids and dicarboxylic acids was similar for all the pigment and linseed oil mixtures. However, it could already be seen from the chromatograms that the concentrations of the mentioned compounds differed. A representative chromatogram is presented in Figure 10. The aged paints contained three main original fatty acids and the most common aging products of drying oils – palmitic (P), stearic (S), oleic (O), azelaic (A), sebacic (Se), suberic (Su), and pimelic acid (Pi). To estimate the within-lab reproducibility of the GC-MS method with the ACM derivatization, one sample was analyzed in replicates – the absolute quantification of the yellow ochre + linseed oil 50 g/100 g mixture on five days over two months yielded in fatty acid average concentrations of P = 1.33 ± 0.05 g; S = 0.86 ± 0.01 g; and O = 0.14 ± 0.03 g per 100 g of dried sample. The P/S ratio was 0.65 ± 0.02. The presented uncertainties are standard deviations of the five measurements. This intermediate precision estimation shows that the ACM procedure is a suitable derivatization method for the samples analyzed in paper III.

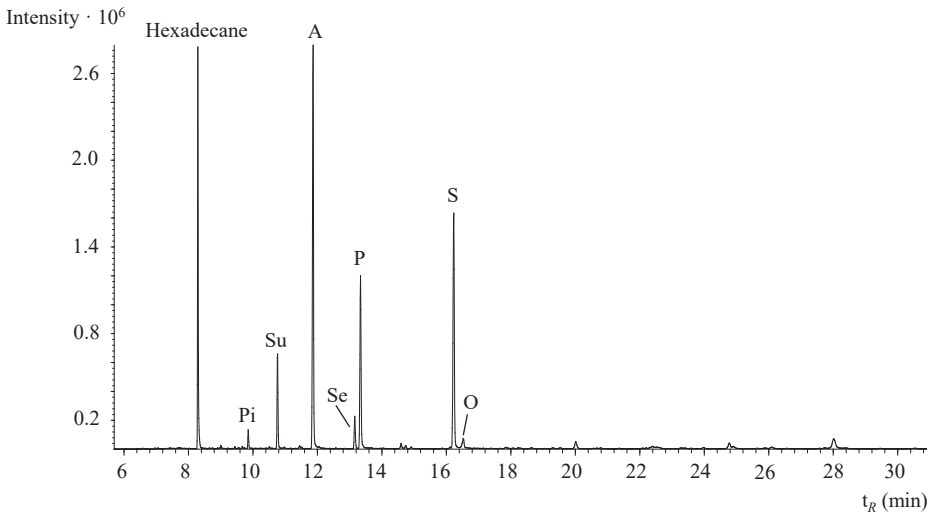

Figure 10. Representative chromatogram recorded in the SIM mode of the aged Prussian blue + linseed oil mixture (50 g/100 g). Hexadecane was used as the internal standard. The abbreviations are explained in the text above.

4.4.1. Relative values of the paint mock-ups

The relative quantification results of the fatty acids and dicarboxylic acids in the aged paint samples are often reported as P/S, A/P, or ∑D values. For fresh linseed oil, these values were respectively found to be 1.5, 0, and 0%. In the paint mock-ups, the average P/S values were 0.7 (Prussian blue + linseed oil), 0.8 (chrome oxide green + linseed oil), 0.9 (natural cinnabar + linseed oil, red ochre + linseed oil), 1.0 (hematite + kaolinite + linseed oil), and 1.5 (yellow ochre + linseed oil, zinc white + linseed oil) even though exactly the same linseed oil had been used in the making of these paints. These results demonstrate that the P/S ratio is not a stable parameter and imply that the extent of palmitic and stearic acid loss from the oil paint is dependent on the type of the pigment. The decrease in the P/S ratio comes from the fact that more palmitic acid has evaporated from the sample compared to stearic acid. Some studies have suggested based on a low P/S value (< 1), that metal stearates may have been added to the paint.[79] In the case of the paints analyzed in paper III, no additional carboxylates were added to these mock-ups, but still, the P/S values are generally below 1. These results raise questions if the drying of other oils (walnut oil, poppy oil) mixed with these pigments would cause the same decrease in the P/S ratio. For example, the P/S value for walnut oil has been reported to be in the range of 2–4.5.[69] A substantial decrease would give a P/S value characteristic to linseed oil (1.4–2.4) and would complicate the differentiation.

It was seen that the type of the pigment influenced the P/S ratio, but the concentration of the pigment did not. However, with A/P and ∑D values the

situation was different. In the case of chrome oxide green, red ochre, yellow ochre, and natural cinnabar oil paint samples, both values increase when the pigment concentration increases – therefore, with these pigments, the concentration has an effect. This implies that even when one pigment + linseed oil paint set was artificially aged in the same conditions, the paints containing more pigment had been more oxidized/dried. Based on the discontinuity of the A/P and ∑D values obtained over the Prussian blue, zinc white, and hematite + kaolinite paint sets it could be concluded that with these pigments, the concentration did not influence the drying processes. Interestingly, these findings do not correlate with the siccative properties of the studied pigments. For example, Prussian blue is a known fast drier; however, the concentration of Prussian blue did not influence the drying extent of the paint mock-ups. On the contrary, the drying extent of the paint set containing cinnabar (a slow drier) was noticeably influenced by the pigment concentration. Especially low values (average values of A/P = 0.3 and ∑D = 13%) were obtained for the zinc white + linseed oil paint set. Based on these results (A/P < 0.3 and ∑D < 15%), some sources would suggest that egg was used as the binding material.[76] However, here we know for certain that linseed oil was used as the binder. Therefore, in similar cases, the A/P and ∑D values could lead to an incorrect characterization.

4.4.2. Absolute quantification of fatty acids in the paint mock-ups

Three original fatty acids (palmitic, stearic, and oleic acid) were present in almost all paint mock-ups, even after aging. The absolute quantities of these fatty acids were calculated (see Table 3 in paper III) and the results of palmitic and stearic acid were placed on a graph (see Figure 11 for stearic acid correlations). Figure 11A contains the results of chrome oxide green, natural cinnabar, Prussian blue, red ochre, and hematite + kaolinite mixtures with linseed oil. Figure 11B shows the results of zinc white and yellow ochre mixtures with linseed oil. If the pigment concentration does not influence the oils' drying processes, then the correlation should be linear. However, Figure 11 demonstrates that this is only the case for the zinc white + linseed oil aged mixtures (R^2 = 0.9921 for the linear trendline). For the other pigment + linseed oil sets, the trendline is far from linear. From Figure 11 it can be inferred that with higher pigment concentration, less stearic acid is left in the sample than one would expect just from the lower oil content.

Therefore, absolute quantification was needed to demonstrate that the lipid composition was affected by the pigment concentration in almost all paint sets (except the zinc white + linseed oil mixtures), even when the relative values (P/S, A/P, and ∑D) did not show any influence from the pigment concentration.

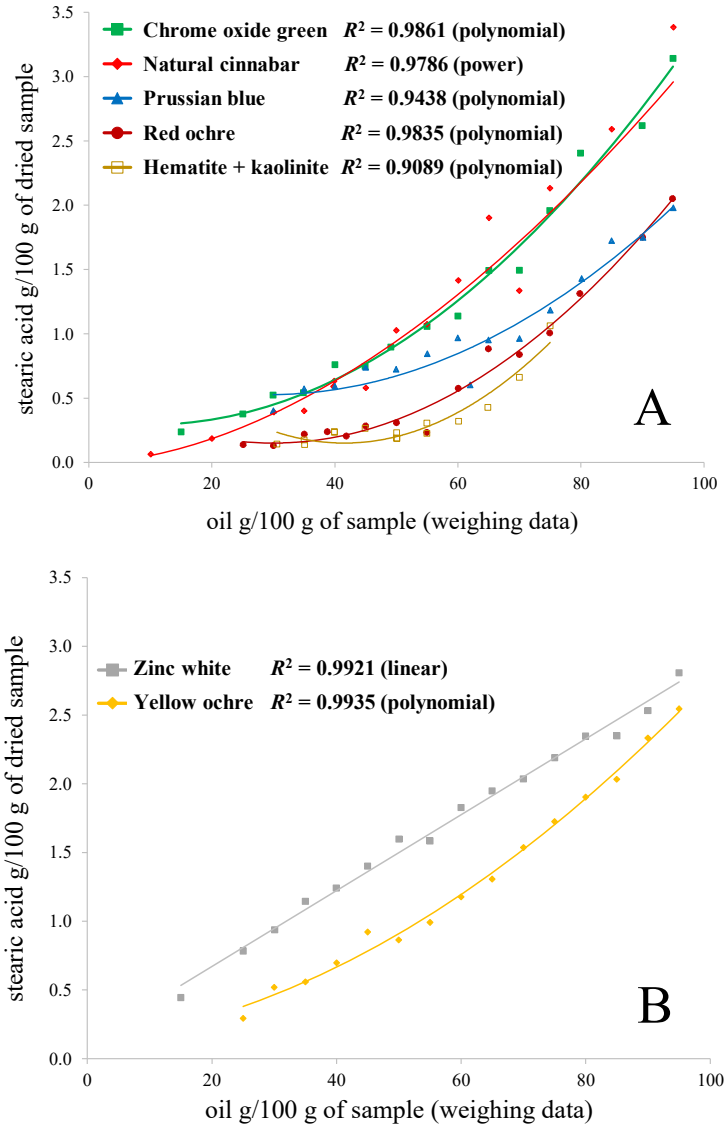

Figure 11. Correlations between stearic acid absolute quantity vs. oil content in the weighted sample. The name of the pigment represents the corresponding pigment + linseed oil mixture.

4.4.3. Comparing some of the GC-MS results with ATR-FT-IR

The stable P/S value, high oleic acid concentration, and low A/P value of the zinc white + linseed oil paint sets can be explained by the formation of metal carboxylates (aka metal soaps) between the metal cation (Zn^{2+}) and the free fatty acids formed during the hydrolysis of TAGs.[34,64,108] The formed metal carboxylates are less prone to evaporate from the drying oil paint than free

carboxylic acids, causing significantly different results than the paint sets containing the other pigments. The presence of zinc soaps was confirmed with the ATR-FT-IR measurements – in the spectrum of zinc white + linseed oil (Figure 12), the absorptions with wavenumbers 1587 cm^{-1} (amorphous structure) and 1539 cm^{-1} (crystalline structure) correspond to zinc carboxylates.[109] Interestingly, around the wavenumber of 1705 cm^{-1}, the zinc white + linseed oil and yellow ochre + linseed oil spectra differ from the spectra of the other pigment + linseed oil mixtures. This absorption corresponds to the C=O stretching, which has been assigned to free carboxylic acids.[110] This absorption is present in all the spectra besides the spectra of zinc white and yellow ochre paint sets. For these two paints sets also the P/S ratio (1.6 and 1.5, respectively) was the closest to the P/S ratio of fresh linseed oil (1.5), which could suggest that the formation of free carboxylic acids is connected to the decrease in the P/S ratio of the other paint sets. Therefore, registering the IR spectrum of the oil paint sample before the GC-MS analysis could give valuable preliminary information about what to expect from the P/S ratio. However, this interesting finding should be investigated more.

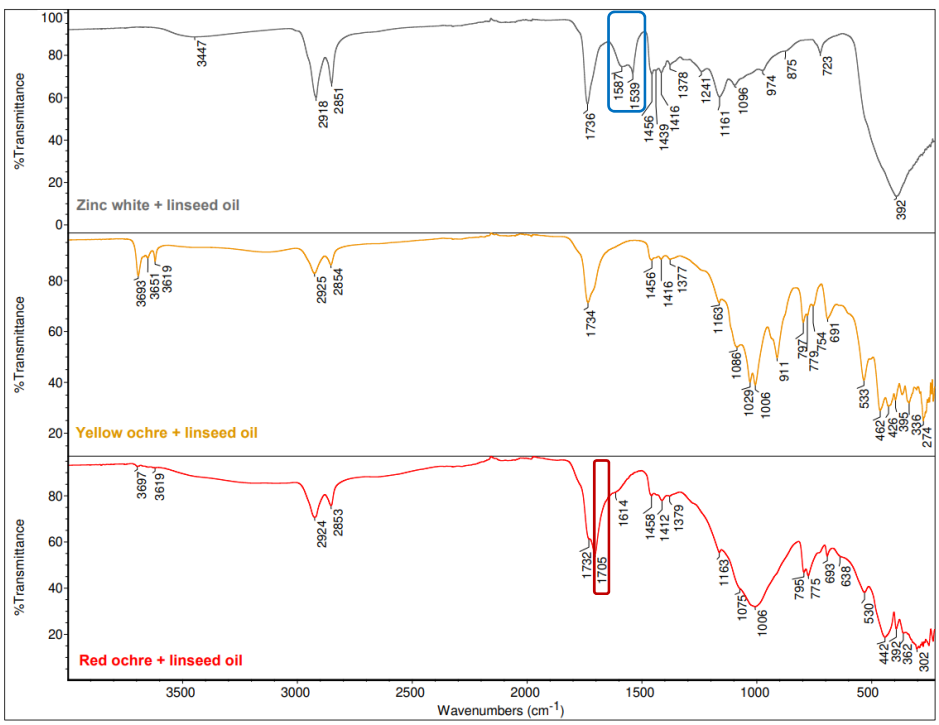

Figure 12. ATR-FT-IR spectra of zinc white, yellow ochre, and red ochre aged oil paint samples (pigment concentration 50 g/100 g). The blue box shows the absorptions corresponding to zinc carboxylates and the red box shows the absorption corresponding to free carboxylic acids.

4.5. Analysis of various samples with the improved methods

Because the objectives of this study were more focused on the systematic characterization of the analysis procedure (i.e., of the pigment concentration effect, the contribution of the derivatization method to the measurement uncertainty, and general comparison of the four derivatization methods), some of the requirements for the analysis of real-life samples were not optimized. For example, the sample amounts available from artifacts are often very low (below 0.1–1 mg) and contain dried (not fresh) oil. Therefore, it would be interesting to compare derivatization methods based on the analysis of smaller amounts of dried oil-paint samples. Of course, then it would not be possible to determine the derivatization efficiencies of the derivatization methods as was the aim in paper I, and the heterogeneity of a dried paint sample would be an issue. However, this analysis could yield valuable information for conservation science regarding which derivatization method is the most efficient (among the compared methods) in derivatizing the analytes in micro samples. In this thesis, higher amounts (10 mg) were used because this enabled the accurate absolute quantification (papers I, III, and analysis of yeast cells), determination of derivatization efficiencies (papers I, II, and analysis of yeast cells), and a better characterization of the overall state of the samples (papers I, III, and analysis of yeast cells). Also, in terms of availability of these samples, the larger sample amounts were not a problem. This thesis demonstrates that different aspects should be considered, and the methods modified accordingly before performing the fatty acid analysis. Next, two applications are presented that both include quantitative analysis but in different ways.

4.5.1. Case study paint samples

The same ACM derivatization used with the GC-MS analysis of artificially aged paint mock-ups was also applied for the analysis of paint samples from two cultural heritage objects relevant to the history of Estonia (Figure 13). One of these artifacts is a 15th century crucifix from Karja church (owner is the EELK Karja Katariina church congregation). Based on written information, in 1924, the crucifix went under conservation and the figure of the Christ was overpainted with white paint. Small pieces from the white overlaying from the perizoma of the Christ were analyzed and the results are discussed in the following sections.

The other artifact is a barn cupboard from Steffens farm located in the Ruhnu island. This cupboard was presumably made at the end of the 18th century or the start of the 19th century. Interestingly, the Ruhnu furniture differs from the traditional farmhouse furniture found elsewhere in Estonia and is nowadays very rare.[111] Small red paint pieces from the top of the cupboard were analyzed and the results are discussed in the following sections.

Figure 13. On the left – crucifix from Karja church (photo: Conservation and Digitisation Centre Kanut); on the right – Cupboard from the Ruhnu island (photo: Kristjan Bachman). The arrows mark the sampling spots.

First, the ATR-FT-IR analysis was performed on both paint samples and the spectra can be seen in Figure 14. The interpretation of the absorption bands demonstrated that the white paint sample from the crucifix of the Karja church contained zinc white as the pigment and gypsum and chalk as fillers. The wavenumbers assigned to the organic medium suggested the presence of an ester-type binding material (possibly oil). Based on the ATR-FT-IR analysis, the red paint sample from the cupboard located on the island of Ruhnu contained red ochre (Fe_2O_3 + kaolinite) as the pigment and maybe chalk as additive. Based on the IR spectrum, the presence of an ester-type binding material (possibly oil) was suggested.

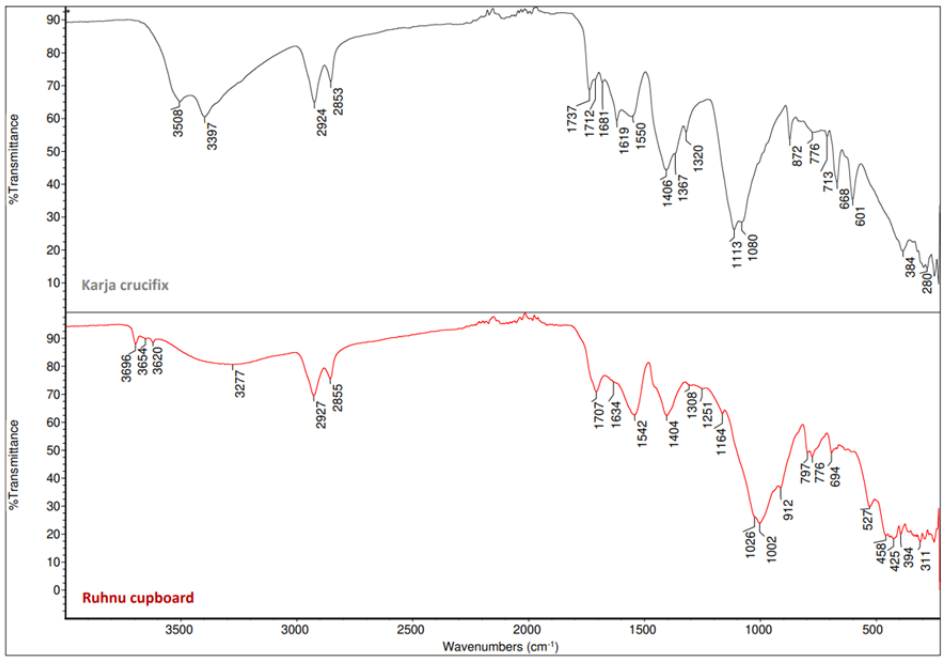

Figure 14. ATR-FT-IR spectra of the white paint sample (crucifix from Karja church) and of the red paint sample (cupboard from the Ruhnu island).

Next, to obtain more information about the ester-type binding material, the GC-MS analysis together with the ACM derivatization was applied to the two case study paint samples. In Figure 15, the recorded total ion chromatograms (TIC) can be seen. For both case study paint samples, the overall lipid profile was essentially the same. However, it could be seen that the relative values of the fatty or dicarboxylic acids varied and therefore, relative quantification was performed. In the case of those samples, the absolute quantification was not possible because the available sample amount was small. However, this was not an issue because, in the present case, the absolute quantification of the fatty acids in those samples would not yield valuable information about the type or condition of the binding material. On the opposite, the comparison of the P/S, A/P, and ∑D values (presented in Table 7) to the corresponding values of the mock-ups might be of value.

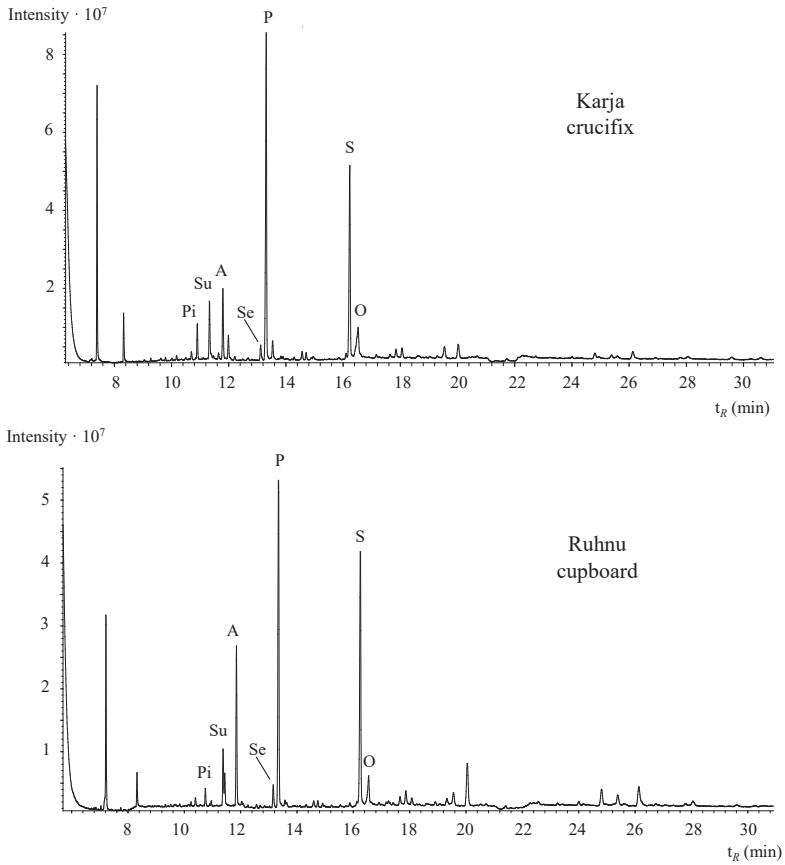

Figure 15. Total ion chromatograms (TIC) of the two case study paint samples, derivatized with the ACM method. The methyl esters of fatty acids and dicarboxylic acids are abbreviated as Pi (pimelic acid), Su (suberic acid), A (azelaic acid), Se (sebacic acid), P (palmitic acid), S (stearic acid), and O (oleic acid).

Table 7. Palmitic to stearic acid ratio (P/S), azelaic to palmitic acid ratio (A/P), and the sum of the relative content of dicarboxylic acids (∑D) calculated from the GC-MS (ACM derivatization) analyses of the case study paint samples.

Crucifix from Karja church			**Ruhnu cupboard**		
P/S	**A/P**	**∑D**	**P/S**	**A/P**	**∑D**
1.6	0.1	7.8	1.2	0.3	13.0

The GC-MS analysis demonstrated especially low A/P and ∑D values for both case study paint samples. As a reminder, values A/P < 0.3 and ∑D < 15% have been used to suggest that the binder is an egg and A/P > 1 together with ∑D > 40% have been used as the evidence for a drying oil binder.[76] Although cholesterol and its degradation products (characteristic to an aged egg binder[112])

were not identified from the lipid analysis and the ATR-FT-IR analysis suggested the use of an ester-type binding material, the presence of egg could not be ruled out because of the low A/P and ∑D values. Therefore, a GC-MS analysis together with the HCl–MTBSTFA procedure developed for the analysis of proteins was performed on both samples. The recorded TIC of both paint samples can be seen in Figure 16.

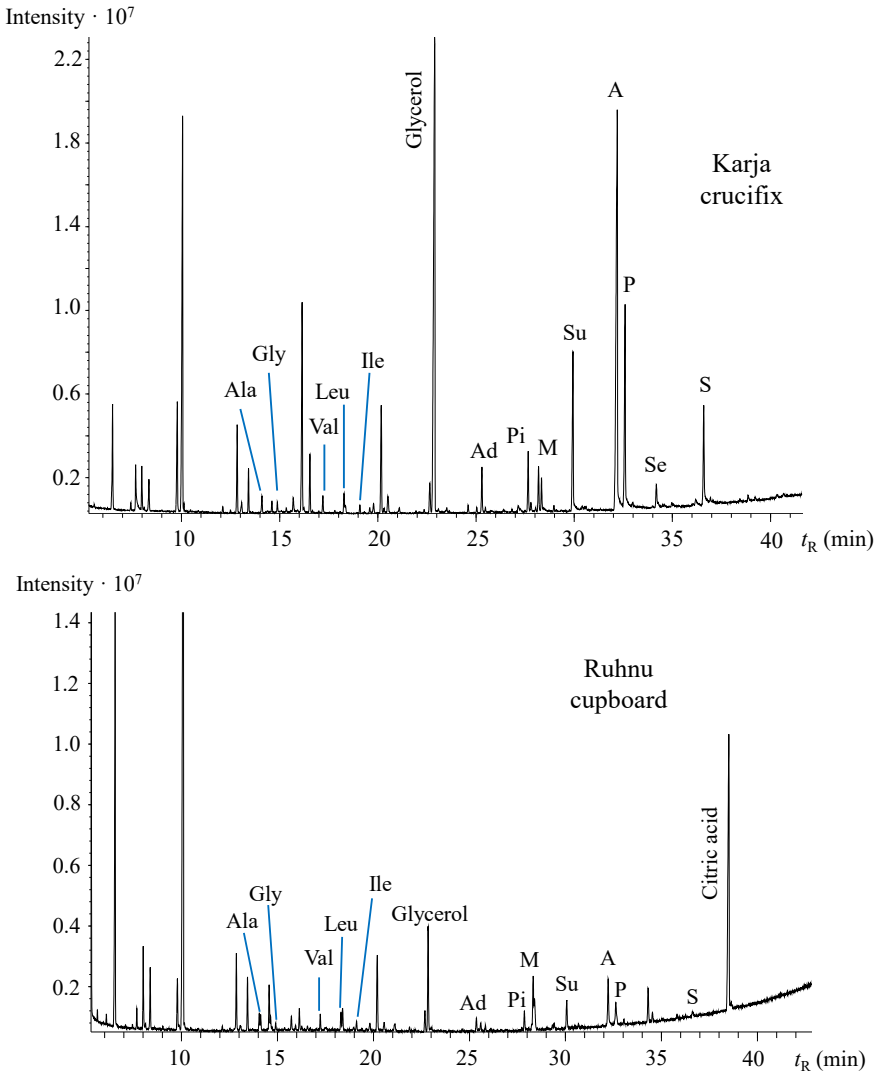

Figure 16. Total ion chromatograms (TIC) of the two case study paint samples, derivatized with the HCl–MTBSTFA method. The following tert-butyldimethylsilyl (TBDMS) derivatives of amino acids were identified: Ala (L-alanine), Gly (glycine), Val (L-valine), Leu (L-leucine), and Ile (isoleucine). The derivatives of fatty acid or dicarboxylic acid are abbreviated as Ad (adipic acid), Pi (pimelic acid), M (myristic acid), Su (suberic acid), A (azelaic acid), P (palmitic acid), Se (sebacic acid), and S (stearic acid).

This derivatization demonstrated that both crucifix from Karja church and Ruhnu cupboard samples contained only small amounts of the derivatives of the following amino acids: L-alanine, glycine, L-valine, L-leucine, and isoleucine. The absence of two amino acids, L-hydroxyproline (characteristic of animal glue) and L-glutamic acid (characteristic of milk and casein), suggest that the paint samples may have contained small amounts of egg.[77] The presence of amino acids does not directly suggest that egg had been mixed with the oil binder. For example, the Karja crucifix had many paint layers, which may have different compositions and are difficult to separate completely from one another. Therefore, the proteins may have originated from an under-layer.

Concerning the P/S ratios obtained with the ACM derivatization, a higher value was calculated for the white paint sample containing zinc white (1.6) and a lower P/S value for the red paint sample containing red ochre (1.2). Because the same derivatization procedure was used to analyze paint mock-ups studied in paper III, some comparisons could be made. The order is in accordance with the average P/S ratios of the mock-ups – for zinc white + linseed oil paint samples P/S = 1.5, for the red ochre + linseed oil paint samples P/S = 0.9, and for the hematite + kaolinite + linseed oil samples P/S = 1.0. Assuming that these samples from the case study objects contained small amounts of egg, then in the case of egg yolk (P/S around 2.2[112]) and linseed oil mixture, the P/S values would be slightly higher, which is in correspondence with the P/S ratios of the case study paint samples. This suggests that linseed oil may have been used as the binding material. However, strong conclusions based on this GC-MS investigation about the presence of linseed oil cannot be made because the origin and type of the used drying oil and the content of an egg is not known. Notably, again the IR spectra of the paint samples (Figure 14) in the range of 1740–1700 cm^{-1} differ. In that range, the red paint sample had one C=O stretching band at 1707 cm^{-1} and the white paint sample two C=O absorptions at 1737 cm^{-1} and 1712 cm^{-1}. As discussed in Section 4.4.3, the absorption near 1705 cm^{-1} corresponds to free fatty acids, which could be why the P/S ratio is lower for the red paint sample. This suggests again that examining the IR spectrum before the GC analysis may give valuable information about the stability of the P/S ratio.

Combining the results of the GC-MS analysis with the two derivatization procedures and the ATR-FT-IR results, it can be concluded that both samples from the two case studies contained mainly oil as the binder and small amounts of amino acids. If the latter originate from egg yolk, then the other ratios (A/P and ∑D) are also affected by the fatty acids originating from the yolk. Interestingly, when calculating the A/P ratios from the GC-MS results of the HCl–MTBSTFA derivatization, much higher values are obtained: 2.6 for the Karja crucifix sample and 1.7 for the Ruhnu sample, which are characteristic for a drying oil (A/P > 1). Therefore, again it was seen that the ratios used to characterize lipid binding materials also depend on the derivatization method (one reason could be different derivatization efficiencies for different fatty and dicarboxylic acids), and that only based on GC-MS analysis and on low A/P

and ∑D values it cannot be interpreted that egg without oil was used as the binder. Also, because the amounts of the case study samples used for the GC-MS analysis were small (around 0.1–0.3 mg), different samples with different compositions may have been taken for the ACM and HCl–MTBSTFA derivatizations. To conclude, the analysis of the case study paint samples suggests again that the values from relative quantification of fatty and dicarboxylic acids can only be used highly judiciously to characterize a lipid-based paint.

4.5.2. Quantification of fatty acids in lyophilized yeast cells

The improved absolute quantification method was also applied for the analysis of fatty acids in yeast cells (*Rhodotorula toruloides* aka *R. toruloides)*. This project is in collaboration with the Food Tech and Bioengineering lab at the Tallinn University of Technology and the results of the GC-MS analysis will be published in an upcoming publication (presumably in 2022). *R. toruloides* is a possible natural starting material for bioproduction because of its ability to synthesize and accumulate high levels of lipids. This renewable resource could be an alternative for fossil fuels to make biofuels and biobased chemicals.[113] The information about the total fatty acid content in the cells was needed to provide experimental input values for developing a model used to characterize the processes taking place during the growing of *R. toruloides* in bioreactors. Knowing the metabolic processes of this yeast could help to improve the design of the microbial cell factories. Because here, the absolute quantities of fatty acids were needed to obtain the overall fatty acid content in the samples, derivatization efficiencies of TAGs (tripalmitin, tristearin, triolein, trilinolein, and trilinolenin) were used to correct the results obtained with the ACM derivatization. Both TIC and SIM chromatograms were recorded from the derivatized samples. In Figure 17, a representative SIM chromatogram of a derivatized yeast cell sample is presented.

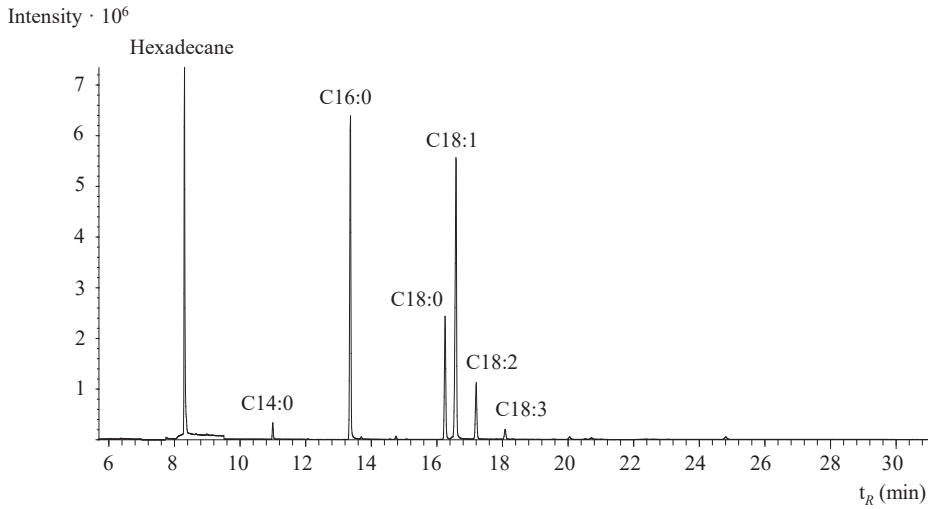

Figure 17. A representative SIM chromatogram of lyophilized yeast cells after derivatization with the ACM method.

Based on the absolute quantification, the total TAG content was found to be in the range of (5.7–48.3)% of the cell dry weight with a relative uncertainty of 16%. The TAG absolute quantification helped to determine that the lipid content in the yeast cells was similar regardless of whether xylose or acetic acid was used as the carbon source. Also, the quantification showed that the lipid content was around 20% during exponential growth phase and around 30% during lipid accumulation phase. The successful analysis of the lyophilized yeast cells demonstrated that the improved quantification method combined with the GC analysis can be applied for the analysis of more diverse samples than just fresh oils or paint layers, ranging from art to bioproduction. However, depending on the research question, limitations, and sample type, the suitable derivatization method (with or without taking derivatization efficiency into account) and overall procedure (qualitative analysis, relative or absolute quantification) need to be chosen.

SUMMARY

The aim of this thesis was to evaluate different GC derivatization methods (based on quantitative analysis) used for the analysis of oils, together with the uncertainty estimation and application of a representative derivatization method for the analysis of samples containing fatty acids.

Four derivatization methods common in cultural heritage and archaeology (TMTFTH, ACM, NaOEt–BSTFA, and KOH–BSTFA) were compared and proved to be suitable for the relative quantification of triglycerides, the main building blocks of oils. However, in terms of absolute quantification, each method had its advantages and disadvantages, and depending on the aims or limitations, different derivatization methods may be applied. The ACM was the cheapest, and for calibration, a commercial mixture of standards can be used. With the NaOEt–BSTFA derivatization, it is possible to perform a separate analysis of free and bounded fatty acids. The KOH–BSTFA has a high derivatization efficiency without the need to use an expensive reagent (as in the case of TMTFTH). However, among the four derivatization methods, TMTFTH was found to be the most suitable for the analysis of fresh oils in terms of derivatization efficiency, intermediate precision, and ease of sample preparation. Regardless of the used derivatization method, it should be assessed if there is a need to include the derivatization efficiency to present the quantitative results accurately.

The two-step KOH–BSTFA derivatization was used to evaluate the uncertainty contribution of the derivatization step with two uncertainty estimation approaches (traditional GUM and MCM). The KOH–BSTFA method was chosen because of its suitability to represent a typical derivatization method. Also, the corresponding calibration curves had the highest scatter, which allows assessing better if taking the correlation between input quantities into account has a noticeable effect. The results showed that in the case of the KOH–BSTFA method, only the derivatization accounted for (7–8)% of relative uncertainty (95% coverage probability), thus being an important contributor to the uncertainty budget of the GC-MS analysis. The MCM approach gave somewhat more realistic uncertainty estimations compared to the traditional GUM approach. Regardless of the applied uncertainty estimation approach, the correlation between input quantities must be accounted for. Otherwise, the uncertainty can be highly overestimated. In the case of the real-life derivatization example studied in this thesis, the overestimation showed to be even (42–50)%.

The GC-MS analysis together with the ACM derivatization (suitable for the absolute quantification of fatty acids in insoluble samples) of the artificially aged pigment and linseed oil mixtures with varying concentrations demonstrated that the widely used values obtained from the relative quantification (P/S, A/P, and ∑D) were influenced both by the pigment type and in some cases also by the pigment concentration. Therefore, these values can only be used highly judiciously when characterizing the type of the used oil or concluding to which

extent the oil paint has dried. The absolute quantification was needed to demonstrate that even when the relative values did not imply that the pigment concentration had an effect, all pigment and linseed oil mixtures studied in this thesis (except for the zinc white paints) were influenced by the pigment concentration. Therefore, the pigment concentration is another important factor needed to be considered when characterizing aged oil paints.

Finally, the developed GC-MS method, together with the ACM derivatization, was applied for the relative quantification of fatty acids present in two case study paint samples from Estonia (white paint sample from Karja crucifix and red paint sample from Ruhnu cupboard). The combined GC-MS analysis showed that both paint samples contained mainly oil as the binder and that the values used to characterize the binder (A/P and $\sum$D) were highly dependent on the derivatization method. Essentially the same method but including absolute quantification and derivatization efficiency was used to find the fatty acid content in lyophilized yeast (*Rhodotorula toruloides*) cells. These absolute quantities of fatty acids were needed to study the metabolic pathways of the growing yeast to move towards a more biobased economy.

REFERENCES

(1) Erhardt, D.; Tumosa, C. S.; Mecklenburg, M. F. Natural and Accelerated Thermal Aging of Oil Paint Films. *Stud. Conserv.* **2000**, *45* (sup1), 65–69. https://doi.org/10.1179/sic.2000.45.Supplement-1.65.

(2) Thomas, A.; Matthäus, B.; Fiebig, H.-J. Fats and Fatty Oils. In *Ullmann's Encyclopedia of Industrial Chemistry*; Wiley-VCH Verlag GmbH & Co. KGaA, 2000. https://doi.org/10.1002/14356007.a10_173.pub2.

(3) Calvano, C. D.; Palmisano, F.; Zambonin, C. G. Laser Desorption/Ionization Time-of-Flight Mass Spectrometry of Triacylglycerols in Oils. *Rapid Commun. Mass Spectrom.* **2005**, *19* (10), 1315–1320. https://doi.org/10.1002/rcm.1933.

(4) Izzo, F. C. *20th Century Artists' Oil Paints: A Chemical-Physical Survey*; PhD thesis; Ca' Foscari University of Venice: Venice, Italy, 2010.

(5) Gandini, A.; Lacerda, T. M.; Carvalho, A. J. F.; Trovatti, E. Progress of Polymers from Renewable Resources: Furans, Vegetable Oils, and Polysaccharides. *Chem. Rev.* **2016**, *116* (3), 1637–1669. https://doi.org/10.1021/acs.chemrev.5b00264.

(6) Méheust, H.; Le Meins, J.-F.; Grau, E.; Cramail, H. Bio-Based Polyricinoleate and Polyhydroxystearate: Properties and Evaluation as Viscosity Modifiers for Lubricants. *ACS Appl. Polym. Mater.* **2021**, *3* (2), 811–818. https://doi.org/10.1021/acsapm.0c01153.

(7) Chakraborty, I.; Chatterjee, K. Polymers and Composites Derived from Castor Oil as Sustainable Materials and Degradable Biomaterials: Current Status and Emerging Trends. *Biomacromolecules* **2020**, *21* (12), 4639–4662. https://doi.org/10.1021/acs.biomac.0c01291.

(8) Wu, J.; Yu, X.; Zhang, H.; Guo, J.; Hu, J.; Li, M.-H. Fully Biobased Vitrimers from Glycyrrhizic Acid and Soybean Oil for Self-Healing, Shape Memory, Weldable, and Recyclable Materials. *ACS Sustain. Chem. Eng.* **2020**, *8* (16), 6479–6487. https://doi.org/10.1021/acssuschemeng.0c01047.

(9) Yara-Varón, E.; Li, Y.; Balcells, M.; Canela-Garayoa, R.; Fabiano-Tixier, A.-S.; Chemat, F. Vegetable Oils as Alternative Solvents for Green Oleo-Extraction, Purification and Formulation of Food and Natural Products. *Molecules* **2017**, *22* (9), 1474. https://doi.org/10.3390/molecules22091474.

(10) Balasubramanian, N.; Steward, K. F. Biodiesel: History of an Innovation to Keep the World Moving. *Substantia* **2019**, 57–71. https://doi.org/10.13128/Substantia-281.

(11) Calvano, C. D.; Ceglie, C. D.; D'Accolti, L.; Zambonin, C. G. MALDI-TOF Mass Spectrometry Detection of Extra-Virgin Olive Oil Adulteration with Hazelnut Oil by Analysis of Phospholipids Using an Ionic Liquid as Matrix and Extraction Solvent. *Food Chem.* **2012**, *134* (2), 1192–1198. https://doi.org/10.1016/j.foodchem.2012.02.154.

(12) Zhang, Y.-L.; Gong, C.; Pei, X.-L.; Han, Y.-L.; Huang, Y.-Y.; Xu, X. Rapid Quantitative Determination of Triglycerides in Edible Oils by Matrix-Assisted Laser Desorption/Ionisation Fourier Transform Ion Cyclotron Resonance Mass Spectrometry Using Pencil Graphite Combined with 2,5-Dihydroxybenzoic Acid as Matrix. *Int. J. Mass Spectrom.* **2018**, *431*, 56–62. https://doi.org/10.1016/j.ijms.2018.06.005.

(13) Chen, T.; Chen, X.; Lu, D.; Chen, B. Detection of Adulteration in Canola Oil by Using GC-IMS and Chemometric Analysis. *Int. J. Anal. Chem.* **2018**, *2018*, e3160265. https://doi.org/10.1155/2018/3160265.

(14) Arslan, F. N.; Akin, G.; Karuk Elmas, Ş. N.; Yilmaz, I.; Janssen, H.-G.; Kenar, A. Rapid Detection of Authenticity and Adulteration of Cold Pressed Black Cumin Seed Oil: A Comparative Study of ATR–FTIR Spectroscopy and Synchronous Fluorescence with Multivariate Data Analysis. *Food Control* **2019**, *98*, 323–332. https://doi.org/10.1016/j.foodcont.2018.11.055.
(15) Ozen, B. F.; Mauer, L. J. Detection of Hazelnut Oil Adulteration Using FT-IR Spectroscopy. *J. Agric. Food Chem.* **2002**, *50* (14), 3898–3901. https://doi.org/10.1021/jf0201834.
(16) Ligor, M.; Buszewski, B. The Comparison of Solid Phase Microextraction-GC and Static Headspace-GC for Determination of Solvent Residues in Vegetable Oils. *J. Sep. Sci.* **2008**, *31* (2), 364–371. https://doi.org/10.1002/jssc.200700303.
(17) Purcaro, G.; Barp, L.; Beccaria, M.; Conte, L. S. Characterisation of Minor Components in Vegetable Oil by Comprehensive Gas Chromatography with Dual Detection. *Food Chem.* **2016**, *212*, 730–738. https://doi.org/10.1016/j.foodchem.2016.06.048.
(18) Zahir, E.; Saeed, R.; Hameed, M. A.; Yousuf, A. Study of Physicochemical Properties of Edible Oil and Evaluation of Frying Oil Quality by Fourier Transform-Infrared (FT-IR) Spectroscopy. *Arab. J. Chem.* **2017**, *10*, S3870–S3876. https://doi.org/10.1016/j.arabjc.2014.05.025.
(19) Tsuzuki, W.; Matsuoka, A.; Ushida, K. Formation of Trans Fatty Acids in Edible Oils during the Frying and Heating Process. *Food Chem.* **2010**, *123* (4), 976–982. https://doi.org/10.1016/j.foodchem.2010.05.048.
(20) van den Berg, J. D. J. *Analytical Chemical Studies on Traditional Linseed Oil Paints*; FOM-Institute for Atomic and Molecular Physics (AMOLF): Amsterdam, The Netherlands, 2002.
(21) Colombini, M. P.; Modugno, F. *Organic Mass Spectrometry in Art and Archaeology*, 1st ed.; John Wiley & Sons, Ltd: Chichester, UK, 2009.
(22) Gettens, R. J.; Stout, G. L. *Painting Materials. A Short Encyclopaedia*, 2nd ed.; Dover Publications, Inc: New York, USA, 1966.
(23) Lazzari, M.; Chiantore, O. Drying and Oxidative Degradation of Linseed Oil. *Polym. Degrad. Stab.* **1999**, *65* (2), 303–313. https://doi.org/10.1016/S0141-3910(99)00020-8.
(24) Degano, I.; La Nasa, J.; Ghelardi, E.; Modugno, F.; Colombini, M. P. Model Study of Modern Oil-Based Paint Media by Triacylglycerol Profiling in Positive and Negative Ionization Modes. *Talanta* **2016**, *161*, 62–70. https://doi.org/10.1016/j.talanta.2016.08.017.
(25) La Nasa, J.; Nodari, L.; Nardella, F.; Sabatini, F.; Degano, I.; Modugno, F.; Legnaioli, S.; Campanella, B.; Tufano, M. K.; Zuena, M.; Tomasin, P. Chemistry of Modern Paint Media: The Strained and Collapsed Painting by Alexis Harding. *Microchem. J.* **2020**, *155*, 104659. https://doi.org/10.1016/j.microc.2020.104659.
(26) Mallégol, J.; Lemaire, J.; Gardette, J.-L. Drier Influence on the Curing of Linseed Oil. *Prog. Org. Coat.* **2000**, *39* (2), 107–113. https://doi.org/10.1016/S0300-9440(00)00126-0.
(27) Mallégol, J.; Gonon, L.; Lemaire, J.; Gardette, J.-L. Long-Term Behaviour of Oil-Based Varnishes and Paints 4. Influence of Film Thickness on the Photooxidation. **2001**, *72*, 191–1997.
(28) Honzíček, J. Curing of Air-Drying Paints: A Critical Review. *Ind. Eng. Chem. Res.* **2019**, *58* (28), 12485–12505. https://doi.org/10.1021/acs.iecr.9b02567.

(29) Seves, A. M.; Sora, S.; Scicolone, G.; Testa, G.; Bonfatti, A. M.; Rossi, E.; Seves, A. Effect of Thermal Accelerated Ageing on the Properties of Model Canvas Paintings. *J. Cult. Herit.* **2000**, *1* (3), 315–322. https://doi.org/10.1016/S1296-2074(00)01078-5.
(30) Colombini, M. P.; Modugno, F.; Menicagli, E.; Fuoco, R.; Giacomelli, A. GC-MS Characterization of Proteinaceous and Lipid Binders in UV Aged Polychrome Artifacts. *Microchem. J.* **2000**, *67* (1–3), 291–300. https://doi.org/10.1016/S0026-265X(00)00075-8.
(31) Modugno, F.; Di Giavincenzo, F.; Degano, I.; van der Werf, I. D.; Bonaduce, I.; van den Berg, K. J. On the Influence of Relative Humidity on the Oxidation and Hydrolysis of Fresh and Aged Oil Paints. *Sci. Rep.* **2019**, *9* (1). http://dx.doi.org/10.1038/s41598-019-41893-9.
(32) Keune, K.; Hoogland, F.; Boon, J. J.; Peggie, D.; Higgit, C. Comparative Study of the Effect of Traditional Pigments on Artificially Aged Oil Paint Systems Using Complementary Analytical Techniques. *Prepr. 15th Trienn. Meet. ICOM Comm. Conserv.* **2008**, *Vol. II*, 833–842.
(33) Tumosa, C. S.; Mecklenburg, M. F. The Influence of Lead Ions on the Drying of Oils. *Stud. Conserv.* **2005**, *50* (sup1), 39–47. https://doi.org/10.1179/sic.2005.50.Supplement-1.39.
(34) Fuster-López, L.; Izzo, F. C.; Piovesan, M.; Yusá-Marco, D. J.; Sperni, L.; Zendri, E. Study of the Chemical Composition and the Mechanical Behaviour of 20th Century Commercial Artists' Oil Paints Containing Manganese-Based Pigments. *Microchem. J.* **2016**, *124*, 962–973. https://doi.org/10.1016/j.microc.2015.08.023.
(35) Cotte, M.; Checroun, E.; Susini, J.; Walter, P. Micro-Analytical Study of Interactions between Oil and Lead Compounds in Paintings. *Appl. Phys. A* **2007**, *89* (4), 841–848. https://doi.org/10.1007/s00339-007-4213-4.
(36) La Nasa, J.; Zanaboni, M.; Uldanck, D.; Degano, I.; Modugno, F.; Kutzke, H.; Tveit, E. S.; Topalova-Casadiego, B.; Colombini, M. P. Novel Application of Liquid Chromatography/Mass Spectrometry for the Characterization of Drying Oils in Art: Elucidation on the Composition of Original Paint Materials Used by Edvard Munch (1863–1944). *Anal. Chim. Acta* **2015**, *896*, 177–189. https://doi.org/10.1016/j.aca.2015.09.023.
(37) Cao, Y.; Suo, Y. Extraction of Microula Sikkimensis Seed Oil and Simultaneous Analysis of Saturated and Unsaturated Fatty Acids by Fluorescence Detection with Reversed-Phase HPLC. *J. Food Compos. Anal.* **2010**, *23* (1), 100–106. https://doi.org/10.1016/j.jfca.2009.07.006.
(38) Bravo, B.; Chávez, G.; Piña, N.; Ysambertt, F.; Márquez, N.; Cáceres, A. Developing an On-Line Derivatization of FAs by Microwave Irradiation Coupled to HPLC Separation with UV Detection. *Talanta* **2004**, *64* (5), 1329–1334. https://doi.org/10.1016/j.talanta.2004.05.022.
(39) Peris Vicente, J.; Gimeno Adelantado, J. V.; Doménech Carbó, M. T.; Mateo Castro, R.; Bosch Reig, F. Identification of Lipid Binders in Old Oil Paintings by Separation of 4-Bromomethyl-7-Methoxycoumarin Derivatives of Fatty Acids by Liquid Chromatography with Fluorescence Detection. *J. Chromatogr. A* **2005**, *1076* (1), 44–50. https://doi.org/10.1016/j.chroma.2005.03.136.
(40) Boukhchina, S.; Gresti, J.; Kallel, H.; Bézard, J. Stereospecific Analysis of TAG from Sunflower Seed Oil. *J. Am. Oil Chem. Soc.* **2003**, *80* (1), 5–8. https://doi.org/10.1007/s11746-003-0641-0.

(41) Dahlberg, D. B.; Lee, S. M.; Wenger, S. J.; Vargo, J. A. Classification of Vegetable Oils by FT-IR. *Appl. Spectrosc.* **1997**, *51* (8), 1118–1124. https://doi.org/10.1366/0003702971941935.
(42) Ng, T.-T.; So, P.-K.; Zheng, B.; Yao, Z.-P. Rapid Screening of Mixed Edible Oils and Gutter Oils by Matrix-Assisted Laser Desorption/Ionization Mass Spectrometry. *Anal. Chim. Acta* **2015**, *884*, 70–76. https://doi.org/10.1016/j.aca.2015.05.013.
(43) Wiesman, Z.; Chapagain, B. P. Determination of Fatty Acid Profiles and TAGs in Vegetable Oils by MALDI-TOF/MS Fingerprinting. In *Lipidomics*; Methods in Molecular Biology; Humana Press, Totowa, NJ, 2009; pp 315–336. https://doi.org/10.1007/978-1-60761-322-0_16.
(44) Berg, J. D. J. van den; Vermist, N. D.; Carlyle, L.; Holčapek, M.; Boon, J. J. Effects of Traditional Processing Methods of Linseed Oil on the Composition of Its Triacylglycerols. *J. Sep. Sci.* **2004**, *27* (3), 181–199. https://doi.org/10.1002/jssc.200301610.
(45) Conceição, J. N.; Marangoni, B. S.; Michels, F. S.; Oliveira, I. P.; Passos, W. E.; Trindade, M. A. G.; Oliveira, S. L.; Caires, A. R. L. Evaluation of Molecular Spectroscopy for Predicting Oxidative Degradation of Biodiesel and Vegetable Oil: Correlation Analysis between Acid Value and UV–Vis Absorbance and Fluorescence. *Fuel Process. Technol.* **2019**, *183*, 1–7. https://doi.org/10.1016/j.fuproc.2018.10.022.
(46) Torrecilla, J. S.; Rojo, E.; Domínguez, J. C.; Rodríguez, F. A Novel Method To Quantify the Adulteration of Extra Virgin Olive Oil with Low-Grade Olive Oils by UV−Vis. *J. Agric. Food Chem.* **2010**, *58* (3), 1679–1684. https://doi.org/10.1021/jf903308u.
(47) Alves, F. C. G. B. S.; Coqueiro, A.; Março, P. H.; Valderrama, P. Evaluation of Olive Oils from the Mediterranean Region by UV–Vis Spectroscopy and Independent Component Analysis. *Food Chem.* **2019**, *273*, 124–129. https://doi.org/10.1016/j.foodchem.2018.01.126.
(48) Ken Sutherland. Gas Chromatography/Mass Spectrometry Techniques for the Characterisation of Organic Materials in Works of Art. *Physical Sciences Review* **2018**.
(49) Hübschmann, H.-J. *Handbook of GC/MS. Fundamentals and Applications*, 2nd ed.; Wiley-VCH Verlag GmbH & Co. KGaA: Weinheim, 2009.
(50) McNair, H. M.; Miller, J. M. *Basic Gas Chromatography. Techniques in Analytical Chemistry*, 2nd ed.; John Wiley & Sons, Inc.: New York, USA, 2009.
(51) Kruve, A.; Rebane, R.; Kipper, K.; Oldekop, M.-L.; Evard, H.; Herodes, K.; Ravio, P.; Leito, I. Tutorial Review on Validation of Liquid Chromatography–Mass Spectrometry Methods: Part I. *Anal. Chim. Acta* **2015**, *870*, 29–44. https://doi.org/10.1016/j.aca.2015.02.017.
(52) Hewavitharana, G. G.; Perera, D. N.; Navaratne, S. B.; Wickramasinghe, I. Extraction Methods of Fat from Food Samples and Preparation of Fatty Acid Methyl Esters for Gas Chromatography: A Review. *Arab. J. Chem.* **2020**, *13* (8), 6865–6875. https://doi.org/10.1016/j.arabjc.2020.06.039.
(53) Calvano, C. D.; van der Werf, I. D.; Palmisano, F.; Sabbatini, L. Revealing the Composition of Organic Materials in Polychrome Works of Art: The Role of Mass Spectrometry-Based Techniques. *Anal. Bioanal. Chem.* **2016**, *408* (25), 6957–6981. https://doi.org/10.1007/s00216-016-9862-8.
(54) Halket, J. M.; Zaikin, V. G. Derivatization in Mass Spectrometry—1. Silylation. *Eur. J. Mass Spectrom.* **2003**, *9* (1), 1–21. https://doi.org/10.1255/ejms.527.

(55) Llorent-Martínez, E. J.; Domínguez-Vidal, A.; Rubio-Domene, R.; Pascual-Reguera, M. I.; Ruiz-Medina, A.; Ayora-Cañada, M. J. Identification of Lipidic Binding Media in Plasterwork Decorations from the Alhambra Using GC–MS and Chemometrics: Influence of Pigments and Aging. *Microchem. J.* **2014**, *115*, 11–18. https://doi.org/10.1016/j.microc.2014.02.001.
(56) Salimon, J.; Omar, T. A.; Salih, N. Comparison of Two Derivatization Methods for the Analysis of Fatty Acids and Trans Fatty Acids in Bakery Products Using Gas Chromatography. *Sci. World J.* **2014**, *vol 2014*, 10 pages. https://doi.org/10.1155/2014/906407.
(57) Stern, B.; Heron, C.; Serpico, M.; Bourriau, J. A Comparison of Methods for Establishing Fatty Acid Concentration Gradients across Potsherds: A Case Study Using Late Bronze Age Canaanite Amphorae*. *Archaeometry* **2000**, *42* (2), 399–414. https://doi.org/10.1111/j.1475-4754.2000.tb00890.x.
(58) Piccirillo, A.; Scalarone, D.; Chiantore, O. Comparison between Off-Line and on-Line Derivatisation Methods in the Characterisation of Siccative Oils in Paint Media. *J. Anal. Appl. Pyrolysis* **2005**, *74* (1–2), 33–38. https://doi.org/10.1016/j.jaap.2004.11.014.
(59) Witkowski, B.; Duchnowicz, A.; Ganeczko, M.; Laudy, A.; Gierczak, T.; Biesaga, M. Identification of Proteins, Drying Oils, Waxes and Resins in the Works of Art Micro-samples by Chromatographic and Mass Spectrometric Techniques. *J. Sep. Sci.* **2018**, *41* (3), 630–638. https://doi.org/10.1002/jssc.201700937.
(60) Sutherland, K. Derivatisation Using M-(Trifluoromethyl)Phenyltrimethylammonium Hydroxide of Organic Materials in Artworks for Analysis by Gas Chromatography–Mass Spectrometry: Unusual Reaction Products with Alcohols. *J. Chromatogr. A* **2007**, *1149* (1), 30–37.
(61) Degano, I.; Modugno, F.; Bonaduce, I.; Ribechini, E.; Colombini, M. P. Recent Advances in Analytical Pyrolysis to Investigate Organic Materials in Heritage Science. *Angew. Chem. Int. Ed.* **2018**, *57* (25), 7313–7323. https://doi.org/10.1002/anie.201713404.
(62) Pitthard, V.; Finch, P.; Bayerová, T. Direct Chemolysis–Gas Chromatography–Mass Spectrometry for Analysis of Paint Materials. *J. Sep. Sci.* **2004**, *27* (3), 200–208. https://doi.org/10.1002/jssc.200301617.
(63) Aldai, N.; Murray, B. E.; Najera, A. I.; Troy, D. J.; Osoro, K. Derivatization of Fatty Acids and Its Application for Conjugated Linoleic Acid Studies in Ruminant Meat Lipids. *J. Sci. Food Agric.* **2005**, No. 85, 1073–1083.
(64) Bonaduce, I.; Carlyle, L.; Colombini, M. P.; Duce, C.; Ferrari, C.; Ribechini, E.; Selleri, P.; Tiné, M. R. New Insights into the Ageing of Linseed Oil Paint Binder: A Qualitative and Quantitative Analytical Study. *PLOS ONE* **2012**, *7* (11), e49333. https://doi.org/10.1371/journal.pone.0049333.
(65) van den Berg, J. D. J.; van den Berg, K. J.; Boon, J. J. Determination of the Degree of Hydrolysis of Oil Paint Samples Using a Two-Step Derivatisation Method and on-Column GC/MS. *Prog. Org. Coat.* **2001**, *41* (1–3), 143–155. https://doi.org/10.1016/S0300-9440(01)00140-0.
(66) Young, K. E.; Quinn, S. M.; Trumble, S. J. Comparing Gas Chromatographic Techniques Used in Fatty Acid Profiling of Northern Fur Seals (Callorhinusursinus) and Steller Seal Lions (Eumetopiasjubatus) from Lovushki Island Complex, Russia. *Int. J. Appl. Sci. Technol.* **2012**, *2* (9), 11–21.
(67) Mills, J. S.; White, R. *The Organic Chemistry of Museum Objects*, 2nd ed.; Elsevier Science Ltd: Oxford, 1994.

(68) Mills, J. S. The Gas Chromatographic Examination of Paint Media. Part I. Fatty Acid Composition and Identification of Dried Oil Films. *Stud. Conserv.* **1966**, No. 11, 92–107. https://doi.org/10.1179/sic.1966.011.
(69) Colombini, M. P.; Andreotti, A.; Bonaduce, I.; Modugno, F.; Ribechini, E. Analytical Strategies for Characterizing Organic Paint Media Using Gas Chromatography/Mass Spectrometry. *Acc. Chem. Res.* **2010**, *43* (6), 715–727. https://doi.org/10.1021/ar900185f.
(70) Pitthard, V.; Stanek, S.; Griesser, M.; Muxeneder, T. Gas Chromatography – Mass Spectrometry of Binding Media from Early 20th Century Paint Samples from Arnold Schönberg's Palette. *Chromatographia* **2005**, *62* (3), 175–182. https://doi.org/10.1365/s10337-005-0595-7.
(71) Cappitelli, F.; Learner, T.; Chiantore, O. An Initial Assessment of Thermally Assisted Hydrolysis and Methylation-Gas Chromatography/Mass Spectrometry for the Identification of Oils from Dried Paint Films. *J. Anal. Appl. Pyrolysis* **2002**, *63* (2), 339–348. https://doi.org/10.1016/S0165-2370(01)00164-4.
(72) Cartoni, G.; Russo, M. V.; Francesca Spinelli; Talarico, F. Characterisation of Fatty Acids in Drying Oils Used in Paintings on Canvas by GC and GC-MS Analysis. *Soc. Chim. Ital.* **2001**, *91* (1), 719–726.
(73) Fuster-López, L.; Izzo, F. C.; Damato, V.; Yusà-Marco, D. J.; Zendri, E. An Insight into the Mechanical Properties of Selected Commercial Oil and Alkyd Paint Films Containing Cobalt Blue. *J. Cult. Herit.* **2019**, *35*, 225–234. https://doi.org/10.1016/j.culher.2018.12.007.
(74) Elsayed, Y. Identification of the Painting Materials of a Unique Easel Painting by Mahmoud Sa'id. *Egypt. J. Archaeol. Restor. Stud.* **2019**, *9* (2), 155–169. https://doi.org/10.21608/ejars.2019.66984.
(75) Schilling, M. R.; Carson, D. M.; Khanjian, H. P. Evaporation of Fatty Acids and the Formation of Ghost Images by Framed Oil Paintings. *WAAC Newsletter*. 21st ed. 1998.
(76) Kalinina, K. B.; Bonaduce, I.; Colombini, M. P.; Artemieva, Irina. S. An Analytical Investigation of the Painting Technique of Italian Renaissance Master Lorenzo Lotto. *J. Cult. Herit.* **2012**, *13* (3), 259–274. https://doi.org/10.1016/j.culher.2011.11.005.
(77) Colombini, M. P.; Modugno, F.; Giacomelli, M.; Francesconi, S. Characterisation of Proteinaceous Binders and Drying Oils in Wall Painting Samples by Gas Chromatography-Mass Spectrometry. *J. Chromatogr. A* **1999**, No. 846, 113–124.
(78) Pitthard, V.; Griesser, M.; Stanek, S. Methodology and Application of GC-MS to Study Altered Organic Binding Media from Objects of the Kunsthistorisches Museum, Vienna. *Ann. Chim.* **2006**, *96* (9–10), 561–573. https://doi.org/10.1002/adic.200690058.
(79) Banti, D.; Nasa, J. L.; Tenorio, A. L.; Modugno, F.; Berg, K. J. van den; Lee, J.; Ormsby, B.; Burnstock, A.; Bonaduce, I. A Molecular Study of Modern Oil Paintings: Investigating the Role of Dicarboxylic Acids in the Water Sensitivity of Modern Oil Paints. *RSC Adv.* **2018**, *8* (11), 6001–6012. https://doi.org/10.1039/C7RA13364B.
(80) La Nasa, J.; Modugno, F.; Aloisi, M.; Lluveras-Tenorio, A.; Bonaduce, I. Development of a GC/MS Method for the Qualitative and Quantitative Analysis of Mixtures of Free Fatty Acids and Metal Soaps in Paint Samples. *Anal. Chim. Acta* **2018**, *1001*, 51–58. https://doi.org/10.1016/j.aca.2017.11.017.

(81) JCGM 200:2008 International Vocabulary of Metrology - Basic and General Concepts and Associated Terms (VIM). 2008.
(82) Meyer, V. R. Measurement Uncertainty. *J. Chromatogr. A* **2007**, *1158* (1), 15–24. https://doi.org/10.1016/j.chroma.2007.02.082.
(83) *Chemical Derivatization in Analytical Chemistry. Volume 1: Chromatography*, Plenum Press.; Frei, R. W., Lawrence, J. F., Eds.; New York, USA, 1981.
(84) de Souza Eller Franco de Oliveira, S. C. W.; Yonamine, M. Measurement Uncertainty for the Determination of Amphetamines in Urine by Liquid-Phase Microextraction and Gas Chromatography-Mass Spectrometry. *265* **2016**, 81–88.
(85) Pagliano, E.; Meija, J.; Mester, Z. High-Precision Quadruple Isotope Dilution Method for Simultaneous Determination of Nitrite and Nitrate in Seawater by GCMS after Derivatization with Triethyloxonium Tetrafluoroborate. *824* **2014**, 36–41.
(86) Ammazzini, S.; Onor, M.; Pagliano, E.; Mester, Z.; Campanella, B.; Pitzalis, E.; Bramanti, E.; D'Ulivo, A. Determination of Thiocyanate in Saliva by Headspace Gas Chromatography-Mass Spectrometry, Following a Single-Step Aqueous Derivatization with Triethyloxonium Tetrafluoroborate. *1400* **2015**, 124–130.
(87) Douny, C.; Tihon, A.; Bayonnet, P.; Brose, F.; Degand, G.; Rozet, E.; Milet, J.; Ribonnet, L.; Lambin, L.; Larondelle, Y.; Scippo, M.-L. Validation of the Analytical Procedure for the Determination of Malondialdehyde and Three Other Aldehydes in Vegetable Oil Using Liquid Chromatography Coupled to Tandem Mass Spectrometry (LC-MS/MS) and Application to Linseed Oil. *8* **2015**, *6*, 1425–1435.
(88) Pagliano, E.; Mester, Z.; Meija, J. Reduction of Measurement Uncertainty by Experimental Design in High-Order (Double, Triple, and Quadruple) Isotope Dilution Mass Spectrometry: Application to GC-MS Measurement of Bromide. *405* **2013**, *9*, 2879–2887.
(89) Bettencourt da Silva, R. J. N. Spreadsheet for Designing Valid Least-Squares Calibrations: A Tutorial. *Talanta* **2016**, *148*, 177–190. https://doi.org/10.1016/j.talanta. 2015.10.072.
(90) Song, J.; Niu, B.; Wang, D.; Zhang, F. Comparison of the Monte Carlo and Guide to Uncertainty in Measurement Methods in Estimating Measurement Uncertainty: Indirect Measurement of the CaMV35S Promoter in Mixed Samples of Genetically Modified Soybean. *Food Control* **2018**, *90*, 131–139. https://doi.org/10.1016/j.foodcont.2018.02.010.
(91) Sega, M.; Pennecchi, F.; Rinaldi, S.; Rolle, F. Uncertainty Evaluation for the Quantification of Low Masses of Benzo[a]Pyrene: Comparison between the Law of Propagation of Uncertainty and the Monte Carlo Method. *Anal. Chim. Acta* **2016**, *920*, 10–17. https://doi.org/10.1016/j.aca.2016.03.032.
(92) Sousa, J. A.; Reynolds, A. M.; Ribeiro, Á. S. A Comparison in the Evaluation of Measurement Uncertainty in Analytical Chemistry Testing between the Use of Quality Control Data and a Regression Analysis. *Accreditation Qual. Assur.* **2012**, *17* (2), 207–214. https://doi.org/10.1007/s00769-011-0874-y.
(93) Theodorou, D.; Meligotsidou, L.; Karavoltsos, S.; Burnetas, A.; Dassenakis, M.; Scoullos, M. Comparison of ISO-GUM and Monte Carlo Methods for the Evaluation of Measurement Uncertainty: Application to Direct Cadmium Measurement in Water by GFAAS. *Talanta* **2011**, *83* (5), 1568–1574. https://doi.org/10.1016/j.talanta.2010.11.059.

(94) Mildenhall, S. J. Correlation and Aggregate Loss Distributions With An Emphasis On The Iman-Conover Method. **2005**, 101.
(95) Nelsen, R. B. *An Introduction to Copulas*, 2nd ed.; Springer Series in Statistics; Springer-Verlag: New York, 2006. https://doi.org/10.1007/0-387-28678-0.
(96) JCGM 100:2008 Evaluation of Measurement Data – Guide to the Expression of Uncertainty in Measurement. 2008.
(97) JCGM 101:2008 Evaluation of Measurement Data – Supplement 1 to the "Guide to the Expression of Uncertainty in Measurement" – Propagation of Distributions Using a Monte Carlo Method. 2008.
(98) Ángeles Herrador, M.; González, A. G. Evaluation of Measurement Uncertainty in Analytical Assays by Means of Monte-Carlo Simulation. *Talanta* **2004**, *64* (2), 415–422. https://doi.org/10.1016/j.talanta.2004.03.011.
(99) Ellison, S. L. R.; Williams, A. EURACHEM / CITAC Guide CG 4. Quantifiying Uncertainty in Analytical Measurement. 2012.
(100) Noda, H.; Bode, J. W. Synthesis and Chemoselective Ligations of MIDA Acylboronates with O-Me Hydroxylamines. *Chem. Sci.* **2014**, *5*, 4328–4332.
(101) Kruve, A.; Rebane, R.; Kipper, K.; Oldekop, M.-L.; Evard, H.; Herodes, K.; Ravio, P.; Leito, I. Tutorial Review on Validation of Liquid Chromatography–Mass Spectrometry Methods: Part II. *Anal. Chim. Acta* **2015**, *870*, 8–28. https://doi.org/10.1016/j.aca.2015.02.016.
(102) Manzano, E.; Rodriguez-Simón, L. R.; Navas, N.; Checa-Moreno, R.; Romero-Gámez, M.; Capitan-Vallvey, L. F. Study of the GC–MS Determination of the Palmitic–Stearic Acid Ratio for the Characterisation of Drying Oil in Painting: La Encarnación by Alonso Cano as a Case Study. *Talanta* **2011**, *84* (4), 1148–1154. https://doi.org/10.1016/j.talanta.2011.03.012.
(103) Lluveras, A.; Bonaduce, I.; Andreotti, A.; Colombini, M. P. GC/MS Analytical Procedure for the Characterization of Glycerolipids, Natural Waxes, Terpenoid Resins, Proteinaceous and Polysaccharide Materials in the Same Paint Microsample Avoiding Interferences from Inorganic Media. *Anal. Chem.* **2010**, *82* (1), 376–386. https://doi.org/10.1021/ac902141m.
(104) Craig, O. E.; Saul, H.; Lucquin, A.; Nishida, Y.; Taché, K.; Clarke, L.; Thompson, A.; Altoft, D. T.; Uchiyama, J.; Ajimoto, M.; Gibbs, K.; Isaksson, S.; Heron, C. P.; Jordan, P. Earliest Evidence for the Use of Pottery. *Nature* **2013**, *496* (7445), 351–354. https://doi.org/10.1038/nature12109.
(105) Pitthard, V.; Griesser, M.; Stanek, S.; Bayerova, T. Study of Complex Organic Binding Media Systems on Artworks Applying GC-MS Analysis: Selected Examples from the Kunsthistorisches Museum, Vienna. *Macromol. Symp.* **2006**, *238* (1), 37–45. https://doi.org/10.1002/masy.200650606.
(106) Bettencourt da Silva, R. J. N. Evaluation of Trace Analyte Identification in Complex Matrices by Low-Resolution Gas Chromatography – Mass Spectrometry through Signal Simulation. *Talanta* **2016**, *150*, 553–567. https://doi.org/10.1016/j.talanta.2015.12.033.
(107) Petersen, P. H.; Stöckl, D.; Westgard, J. O.; Sandberg, S.; Linnet, K.; Thienpont, L. Models for Combining Random and Systematic Errors. Assumptions and Consequences for Different Models. **2001**, *39* (7), 589–595. https://doi.org/10.1515/CCLM.2001.094.
(108) Osmond, G. Zinc White: A Review of Zinc Oxide Pigment Properties and Implications for Stability in Oil-Based Paintings. *AICCM Bull.* **2012**, *33* (1), 20–29. https://doi.org/10.1179/bac.2012.33.1.004.

(109) J. Hermans, J.; Keune, K.; Loon, A. van; D. Iedema, P. An Infrared Spectroscopic Study of the Nature of Zinc Carboxylates in Oil Paintings. *J. Anal. At. Spectrom.* **2015**, *30* (7), 1600–1608. https://doi.org/10.1039/C5JA00120J.
(110) van der Weerd, J.; van Loon, A.; Boon, J. J. FTIR Studies of the Effects of Pigments on the Aging of Oil. *Stud. Conserv.* **2005**, *50* (1), 3–22. https://doi.org/10.1179/sic.2005.50.1.3.
(111) Bachman, K. The connections between Ruhnu farm furniture and carpentry tools. *Stud. Vernacula* **2017**, *8*, 122–139.
(112) Colombini, M. P.; Modugno, F.; Fuoco, R.; Tognazzi, A. A GC-MS Study on the Deterioration of Lipidic Paint Binders. *Microchem. J.* **2002**, *73* (1), 175–185. https://doi.org/10.1016/S0026-265X(02)00062-0.
(113) Park, Y.-K.; Nicaud, J.-M.; Ledesma-Amaro, R. The Engineering Potential of Rhodosporidium Toruloides as a Workhorse for Biotechnological Applications. *Trends Biotechnol.* **2018**, *36* (3), 304–317. https://doi.org/10.1016/j.tibtech.2017.10.013.

SUMMARY IN ESTONIAN

Õlide derivatiseerimine ja kvantitatiivne gaasikromatograafiline analüüs

Käesoleva doktoritöö eesmärgiks oli uurida gaasikromatograafia (GC) derivatiseerimismetoodikate sobilikkust taimeõlide kvantitatiivseks analüüsiks, hinnata derivatiseerimise mõõtemääramatust ning rakendada väljatöötatud metoodikaid rasvhapete kvantitatiivseks analüüsiks erinevates proovides.

Derivatiseerimismetoodikate võrdlus näitas, et kõik neli metoodikat (TMTFTH, ACM, NaOEt–BSTFA ja KOH–BSTFA), mis on laialt levinud kultuuriväärtuste ja/või arheoloogiliste objektide analüüsis, on sobilikud triglütseriidide suhteliseks kvantiseerimiseks värsketes õlides. Metoodikad ei olnud aga võrdväärsed absoluutses kvantiseerimises, mistõttu sõltuvalt analüüsi eesmärgist või piirangutest tuleks vajadusel enne hinnata milline on sobiv derivatiseerimismetoodika. Nelja metoodika võrdluses oli igal derivatiseerimisel omad eelised ja ka puudused. ACM on kõige odavam, reagendid on tavalaborites olemas ja kalibreerimiseks on võimalik kasutada kommertsiaalselt kättesaadavaid standardeid. NaOEt–BSTFA derivatiseerimine võimaldab analüüsida eraldi vabu ja seotuid rasvhappeid. KOH–BSTFA meetod on kõrge derivatiseerimisefektiivsusega ning reagendid on odavamad kui TMTFTH meetodi omad. Derivatiseerimisefektiivsuse, laborisisese korratavuse ja prooviettevalmistuse põhjal oli nelja meetodi seas värsketele õlidele rakendatuna kõige edukam TMTFTH derivatiseerimine. Absoluutne kvantiseerimine näitas, et sõltumata derivatiseerimismeetodist (kuid sõltuvalt analüüsi eesmärgist ja tulemusena esitatavast suurusest) tuleks eelnevalt hinnata millised on derivatiseerimisefektiivsuse väärtuseid ja kas neid oleks vaja kaasata korrektse analüüsitulemuse esitamisel.

Derivatiseerimise mõõtemääramatuse hindamiseks kasutati ning võrreldi kahte lähenemist – traditsioonilist komponentidepõhist GUM lähenemist ja Monte Carlo simulatsiooni (MCM). Kahe-etapiline KOH–BSTFA derivatiseerimine valiti esindama tüüpilist derivatiseerimismetoodikat. Kuna sellele metoodikale vastavate kalibreerimisgraafikute punktid olid kõige suuremate hajuvustega leiti, et selle abil on parim hinnata sisendsuuruste korrelatsiooni arvestamise või mittearvestamise mõju lõppväärtusele. Tulemused näitasid, et KOH–BSTFA meetodi puhul oli 95% katteteguri juures derivatiseerimisest tulenev suhteline mõõtemääramatus (7–8)%. Seega on derivatiseerimine üks olulisemaid mõõtemääramatuse allikaid GC analüüsis. Kahe lähenemise võrdlus näitas, et võrreldes traditsioonilise GUM lähenemisega on MCM lähenemisega saadud mõõtemääramatuse hinnangud ainult vähesel määral realistlikumad. Sisendsuuruste korrelatsiooni analüüs aga näitas, et sõltumata kasutatavast mõõtemääramatuse hindamise meetodist tuleb korrelatsiooni olemasolu korral see arvesse võtta. Vastasel juhul võib arvutatud mõõtemääramatus olla suuresti ülehinnatud – käesolevas töös isegi kuni 50%.

Väljatöötatud GC-MS metoodikat rakendati koos ACM derivatiseerimisega (võimaldab viia läbi rasvhapete absoluutset kvantiseerimist halvasti lahustu-

vates proovides) erinevate proovide analüüsiks. Kunstlikult vanandatud pigmendi ja linaseemneõli värviproovidele viidi läbi nii suhteline kui ka absoluutne kvantiseerimine. Tulemused näitasid, et suhtelisel kvantiseerimisel saadud suurused (P/S, A/P ja ∑D), mis on laialt levinud õlide karakteriseerimisel, sõltusid nii pigmendi tüübist kuid mõnel juhul ka pigmendi kontsentratsioonist. Järelikult saab nende suuruste põhjal – vastupidiselt üldlevinud seisukohtadele – ainult äärmiselt kaalutletult karakteriseerida õlitüüpi või kuivamise määra. Absoluutne kvantiseerimine aga näitas, et isegi juhul kui suhtelised väärtused ei viidanud pigmendi kontsentratsiooni mõjule, siis enamikul juhtudest (v.a. tsinkvalge + linaseemneõli proovid) oli kontsentratsiooni mõju õli kuivamisele olemas. Seega on pigmendi kontsentratsioon pealekantavas värvis järjekordne oluline faktor millega tuleb arvestada õlivärvi karakteriseerimisel.

Viimaks rakendati GC-MS meetodit koos ACM derivatiseerimisega kahe reaalse värviproovi koostises olevate rasvhapete suhteliseks kvantiseerimiseks (valge värviproov Karja kiriku krutsifiksilt ja punane värviproov Ruhnu aidakapilt). GC-MS analüüsid näitasid, et mõlemas värviproovis oli peamiseks sideaineks õli. Lisaks demonstreeris kahe derivatiseerimismetoodika kasutamine, et suhted mida kasutatakse sideaine karakteriseerimiseks (A/P ja ∑D) sõltuvad kasutatud derivatiseerimisest. Sama meetodit kuid koos absoluutse kvantiseerimisega rakendati rasvhapete sisalduse leidmiseks lüofiliseeritud pärmirakkudes (*Rhodotorula toruloides*), kus võeti arvesse ka derivatiseerimise efektiivsust. Rasvhapete sisalduse teadmine erinevalt kasvatatud pärmirakkudes on vajalik *R. toruloides* ainevahetusraja uurimiseks, et seda looduslikku ressurssi oleks võimalik kasutada erinevate bioproduktide tootmisel.

ACKNOWLEDGEMENTS

First of all, I would like to express my deepest gratitude to my supervisors professor Ivo Leito and Dr. Signe Vahur for their support and guidance over the years as well as for always encouraging me to act on my ideas. I would also like to thank Siim Salmar for helping with the technical issues of the GC, regardless of the time of the day. My gratitude goes to my friends and colleagues from the Chair of Analytical Chemistry and to all the co-authors, especially Koit Herodes, Anu Teearu-Ojakäär, Martin Vilbaste, Ali Ghiami-Shomami, Mihkel Ilisson, and Sofja Tšepelevitš for your help with the topics of this thesis but also with the other projects that were a big part of my doctoral studies.

My greatest gratitude goes also to Pilleriin Peets and Helen Sepman – thanks for keeping me motivated, ambitious, positive, and for always being there (even as far as from Stockholm and Seoul). Also, I would like to thank all my friends from the organizations Teadusbuss and Keemia Õpikojad. Your enthusiasm for chemistry, experimenting, and teaching has been contagious and shaped me into the person I am today. Finally, I thank my mom for being the greatest family during my studies.

This work has been supported by the Personal Research Funding PUT1521, Personal Research Funding: Team Grant PRG1198, and by the Institutional Research Grants IUT20-14 and IUT20-15 from the Estonian Research Council as well as by the EU through the European Regional Development Fund (TK141 "Advanced materials and high-technology devices for energy recuperation systems" 2014-2020.4.01.15-0011). Also, by the graduate school "Functional materials and technologies", funding from the European Social Fund under Project 1.2.0401.09-0079 in Estonia. This work was carried out using the instrumentation of the Estonian Center of Analytical Chemistry (http://www.akki.ee).

PUBLICATIONS

CURRICULUM VITAE

Name: Eliise Tammekivi
Date of birth: October 22, 1993, Viljandi, Estonia
Citizenship: Estonia
Contact: Institute of Chemistry, University of Tartu, Ravila 14a, 50411, Tartu, Estonia
E-mail: eliise.tammekivi@ut.ee

Education:

2017–…	University of Tartu, chemistry, PhD student
2015–2017	University of Tartu, chemistry, MSc, *cum laude*
2012–2015	University of Tartu, chemistry, BSc, *cum laude*

Professional employment:

2020–…	Chemist, University of Tartu, Institute of Chemistry
2019	Specialist, University of Tartu, Institute of Chemistry
2019–2020	Lecturer, Estonian University of Life Sciences, Institute of Veterinary Medicine and Animal Sciences
2016–2017	Editor (chemistry), AS BIT (Publishing House Avita)

Scientific publications:

1. **Tammekivi, E.**; Vahur, S.; Kekišev, O.; van der Werf, I. D.; Toom, L.; Herodes, K.; Leito, I. Comparison of derivatization methods for the quantitative gas chromatographic analysis of oils. *Analytical Methods*, **2019**, *11* (28), 3514–3522. DOI:10.1039/c9ay00954j.
2. Vilbaste, M.; **Tammekivi, E.**; Leito, I. Uncertainty contribution of derivatization in gas chromatography/mass spectrometric analysis. *Rapid Communications in Mass Spectrometry*, **2020**, *34* (16), e8704. DOI: 10.1002/rcm.8704.
3. **Tammekivi, E.**; Vahur, S.; Vilbaste, M.; Leito, I. Quantitative GC–MS analysis of artificially aged paints with variable pigment and linseed oil ratios. *Molecules*, **2021**, *26* (8), 2218. DOI: 10.3390/molecules26082218
4. **Tammekivi, E.**; Ghiami-Shomami, A.; Tšepelevitš, S.; Trummal, A.; Ilisson, M.; Selberg, S.; Vahur, S.; Teearu, A.; Lõkov, M.; Peets, P.; Pagano, T.; Leito, I. Experimental and Computational Study of Aminoacridines as MALDI(–)-MS Matrix Materials for the Analysis of Complex Samples. *Journal of the American Society for Mass Spectrometry*, **2021**, *32* (4), 1080–1095. DOI: 10.1021/jasms.1c00037.
5. Ghiami-Shomami, A.; **Tammekivi, E.**; Tšepelevitš, S.; Ilisson, M.; Mastitski, A.; Kütt, A.; Toom, L.; Leito, I. Solubility of mono-Aminoacridines: Measurements and Predictions. *Manuscript in preparation*.
6. Rekena, A.; Pinheiro, M.; Bonturi, N.; Belouah, I.; **Tammekivi, E.**; Herodes, K.; Kerkhoven, E.; Lahtvee, P.-J. Enzyme-constrained genome-scale metabolic model of Rhodotorula toruloides. *Manuscript in preparation*.

ELULOOKIRJELDUS

Nimi: Eliise Tammekivi
Sünniaeg: 22. oktoober 1993, Viljandi, Eesti
Kodakonsus: Eesti
Kontakt: Tartu Ülikooli keemia instituut, Ravila 14a, 50411, Tartu, Eesti
E-post: eliise.tammekivi@ut.ee

Haridus:

2017–…	Tartu Ülikool, keemia, doktoriõpe
2015–2017	Tartu Ülikool, keemia, magistriõpe, *cum laude*
2012–2015	Tartu Ülikool, keemia, bakalaureuseõpe, *cum laude*

Töökogemus:

2020–…	Keemik, Tartu Ülikool, keemia instituut
2019	Veebispetsialist, Tartu Ülikool, keemia instituut
2019–2020	Lektor, Eesti Maaülikool, Veterinaarmeditsiini ja loomakasvatuse instituut
2016 – 2017	Toimetaja (keemia), AS BIT (Kirjastus Avita)

Teaduspublikatsioonid:

1. **Tammekivi, E.**; Vahur, S.; Kekišev, O.; van der Werf, I. D.; Toom, L.; Herodes, K.; Leito, I. Comparison of derivatization methods for the quantitative gas chromatographic analysis of oils. *Analytical Methods*, **2019**, *11* (28), 3514–3522. DOI:10.1039/c9ay00954j.
2. Vilbaste, M.; **Tammekivi, E.**; Leito, I. Uncertainty contribution of derivatization in gas chromatography/mass spectrometric analysis. *Rapid Communications in Mass Spectrometry*, **2020**, *34* (16), e8704. DOI: 10.1002/rcm.8704.
3. **Tammekivi, E.**; Vahur, S.; Vilbaste, M.; Leito, I. Quantitative GC–MS analysis of artificially aged paints with variable pigment and linseed oil ratios. *Molecules*, **2021**, *26* (8), 2218. DOI: 10.3390/molecules26082218
4. **Tammekivi, E.**; Ghiami-Shomami, A.; Tšepelevitš, S.; Trummal, A.; Ilisson, M.; Selberg, S.; Vahur, S.; Teearu, A.; Lõkov, M.; Peets, P.; Pagano, T.; Leito, I. Experimental and Computational Study of Aminoacridines as MALDI(–)-MS Matrix Materials for the Analysis of Complex Samples. *Journal of the American Society for Mass Spectrometry*, **2021**, *32* (4), 1080–1095. DOI: 10.1021/jasms.1c00037.
5. Ghiami-Shomami, A.; **Tammekivi, E.**; Tšepelevitš, S.; Ilisson, M.; Mastitski, A.; Kütt, A.; Toom, L.; Leito, I. Solubility of mono-Aminoacridines: Measurements and Predictions. *Manuscript in preparation*.
6. Rekena, A.; Pinheiro, M.; Bonturi, N.; Belouah, I.; **Tammekivi, E.**; Herodes, K.; Kerkhoven, E.; Lahtvee, P.-J. Enzyme-constrained genome-scale metabolic model of Rhodotorula toruloides. *Manuscript in preparation*.

DISSERTATIONES CHIMICAE UNIVERSITATIS TARTUENSIS

1. **Toomas Tamm.** Quantum-chemical simulation of solvent effects. Tartu, 1993, 110 p.
2. **Peeter Burk.** Theoretical study of gas-phase acid-base equilibria. Tartu, 1994, 96 p.
3. **Victor Lobanov.** Quantitative structure-property relationships in large descriptor spaces. Tartu, 1995, 135 p.
4. **Vahur Mäemets.** The ^{17}O and ^{1}H nuclear magnetic resonance study of H_2O in individual solvents and its charged clusters in aqueous solutions of electrolytes. Tartu, 1997, 140 p.
5. **Andrus Metsala.** Microcanonical rate constant in nonequilibrium distribution of vibrational energy and in restricted intramolecular vibrational energy redistribution on the basis of slater's theory of unimolecular reactions. Tartu, 1997, 150 p.
6. **Uko Maran.** Quantum-mechanical study of potential energy surfaces in different environments. Tartu, 1997, 137 p.
7. **Alar Jänes.** Adsorption of organic compounds on antimony, bismuth and cadmium electrodes. Tartu, 1998, 219 p.
8. **Kaido Tammeveski.** Oxygen electroreduction on thin platinum films and the electrochemical detection of superoxide anion. Tartu, 1998, 139 p.
9. **Ivo Leito.** Studies of Brønsted acid-base equilibria in water and non-aqueous media. Tartu, 1998, 101 p.
10. **Jaan Leis.** Conformational dynamics and equilibria in amides. Tartu, 1998, 131 p.
11. **Toonika Rinken.** The modelling of amperometric biosensors based on oxidoreductases. Tartu, 2000, 108 p.
12. **Dmitri Panov.** Partially solvated Grignard reagents. Tartu, 2000, 64 p.
13. **Kaja Orupõld.** Treatment and analysis of phenolic wastewater with microorganisms. Tartu, 2000, 123 p.
14. **Jüri Ivask.** Ion Chromatographic determination of major anions and cations in polar ice core. Tartu, 2000, 85 p.
15. **Lauri Vares.** Stereoselective Synthesis of Tetrahydrofuran and Tetrahydropyran Derivatives by Use of Asymmetric Horner-Wadsworth-Emmons and Ring Closure Reactions. Tartu, 2000, 184 p.
16. **Martin Lepiku.** Kinetic aspects of dopamine D_2 receptor interactions with specific ligands. Tartu, 2000, 81 p.
17. **Katrin Sak.** Some aspects of ligand specificity of P2Y receptors. Tartu, 2000, 106 p.
18. **Vello Pällin.** The role of solvation in the formation of iotsitch complexes. Tartu, 2001, 95 p.
19. **Katrin Kollist.** Interactions between polycyclic aromatic compounds and humic substances. Tartu, 2001, 93 p.

20. **Ivar Koppel.** Quantum chemical study of acidity of strong and superstrong Brønsted acids. Tartu, 2001, 104 p.
21. **Viljar Pihl.** The study of the substituent and solvent effects on the acidity of OH and CH acids. Tartu, 2001, 132 p.
22. **Natalia Palm.** Specification of the minimum, sufficient and significant set of descriptors for general description of solvent effects. Tartu, 2001, 134 p.
23. **Sulev Sild.** QSPR/QSAR approaches for complex molecular systems. Tartu, 2001, 134 p.
24. **Ruslan Petrukhin.** Industrial applications of the quantitative structure-property relationships. Tartu, 2001, 162 p.
25. **Boris V. Rogovoy.** Synthesis of (benzotriazolyl)carboximidamides and their application in relations with *N*- and *S*-nucleophyles. Tartu, 2002, 84 p.
26. **Koit Herodes.** Solvent effects on UV-vis absorption spectra of some solvatochromic substances in binary solvent mixtures: the preferential solvation model. Tartu, 2002, 102 p.
27. **Anti Perkson.** Synthesis and characterisation of nanostructured carbon. Tartu, 2002, 152 p.
28. **Ivari Kaljurand.** Self-consistent acidity scales of neutral and cationic Brønsted acids in acetonitrile and tetrahydrofuran. Tartu, 2003, 108 p.
29. **Karmen Lust.** Adsorption of anions on bismuth single crystal electrodes. Tartu, 2003, 128 p.
30. **Mare Piirsalu.** Substituent, temperature and solvent effects on the alkaline hydrolysis of substituted phenyl and alkyl esters of benzoic acid. Tartu, 2003, 156 p.
31. **Meeri Sassian.** Reactions of partially solvated Grignard reagents. Tartu, 2003, 78 p.
32. **Tarmo Tamm.** Quantum chemical modelling of polypyrrole. Tartu, 2003. 100 p.
33. **Erik Teinemaa.** The environmental fate of the particulate matter and organic pollutants from an oil shale power plant. Tartu, 2003. 102 p.
34. **Jaana Tammiku-Taul.** Quantum chemical study of the properties of Grignard reagents. Tartu, 2003. 120 p.
35. **Andre Lomaka.** Biomedical applications of predictive computational chemistry. Tartu, 2003. 132 p.
36. **Kostyantyn Kirichenko.** Benzotriazole – Mediated Carbon–Carbon Bond Formation. Tartu, 2003. 132 p.
37. **Gunnar Nurk.** Adsorption kinetics of some organic compounds on bismuth single crystal electrodes. Tartu, 2003, 170 p.
38. **Mati Arulepp.** Electrochemical characteristics of porous carbon materials and electrical double layer capacitors. Tartu, 2003, 196 p.
39. **Dan Cornel Fara.** QSPR modeling of complexation and distribution of organic compounds. Tartu, 2004, 126 p.
40. **Riina Mahlapuu.** Signalling of galanin and amyloid precursor protein through adenylate cyclase. Tartu, 2004, 124 p.

41. **Mihkel Kerikmäe.** Some luminescent materials for dosimetric applications and physical research. Tartu, 2004, 143 p.
42. **Jaanus Kruusma.** Determination of some important trace metal ions in human blood. Tartu, 2004, 115 p.
43. **Urmas Johanson.** Investigations of the electrochemical properties of polypyrrole modified electrodes. Tartu, 2004, 91 p.
44. **Kaido Sillar.** Computational study of the acid sites in zeolite ZSM-5. Tartu, 2004, 80 p.
45. **Aldo Oras.** Kinetic aspects of dATPαS interaction with $P2Y_1$ receptor. Tartu, 2004, 75 p.
46. **Erik Mölder.** Measurement of the oxygen mass transfer through the air-water interface. Tartu, 2005, 73 p.
47. **Thomas Thomberg.** The kinetics of electroreduction of peroxodisulfate anion on cadmium (0001) single crystal electrode. Tartu, 2005, 95 p.
48. **Olavi Loog.** Aspects of condensations of carbonyl compounds and their imine analogues. Tartu, 2005, 83 p.
49. **Siim Salmar.** Effect of ultrasound on ester hydrolysis in aqueous ethanol. Tartu, 2006, 73 p.
50. **Ain Uustare.** Modulation of signal transduction of heptahelical receptors by other receptors and G proteins. Tartu, 2006, 121 p.
51. **Sergei Yurchenko.** Determination of some carcinogenic contaminants in food. Tartu, 2006, 143 p.
52. **Kaido Tämm.** QSPR modeling of some properties of organic compounds. Tartu, 2006, 67 p.
53. **Olga Tšubrik.** New methods in the synthesis of multisubstituted hydrazines. Tartu. 2006, 183 p.
54. **Lilli Sooväli.** Spectrophotometric measurements and their uncertainty in chemical analysis and dissociation constant measurements. Tartu, 2006, 125 p.
55. **Eve Koort.** Uncertainty estimation of potentiometrically measured ph and pK_a values. Tartu, 2006, 139 p.
56. **Sergei Kopanchuk.** Regulation of ligand binding to melanocortin receptor subtypes. Tartu, 2006, 119 p.
57. **Silvar Kallip.** Surface structure of some bismuth and antimony single crystal electrodes. Tartu, 2006, 107 p.
58. **Kristjan Saal.** Surface silanization and its application in biomolecule coupling. Tartu, 2006, 77 p.
59. **Tanel Tätte.** High viscosity $Sn(OBu)_4$ oligomeric concentrates and their applications in technology. Tartu, 2006, 91 p.
60. **Dimitar Atanasov Dobchev**. Robust QSAR methods for the prediction of properties from molecular structure. Tartu, 2006, 118 p.
61. **Hannes Hagu**. Impact of ultrasound on hydrophobic interactions in solutions. Tartu, 2007, 81 p.
62. **Rutha Jäger.** Electroreduction of peroxodisulfate anion on bismuth electrodes. Tartu, 2007, 142 p.

63. **Kaido Viht.** Immobilizable bisubstrate-analogue inhibitors of basophilic protein kinases: development and application in biosensors. Tartu, 2007, 88 p.
64. **Eva-Ingrid Rõõm.** Acid-base equilibria in nonpolar media. Tartu, 2007, 156 p.
65. **Sven Tamp.** DFT study of the cesium cation containing complexes relevant to the cesium cation binding by the humic acids. Tartu, 2007, 102 p.
66. **Jaak Nerut.** Electroreduction of hexacyanoferrate(III) anion on Cadmium (0001) single crystal electrode. Tartu, 2007, 180 p.
67. **Lauri Jalukse.** Measurement uncertainty estimation in amperometric dissolved oxygen concentration measurement. Tartu, 2007, 112 p.
68. **Aime Lust.** Charge state of dopants and ordered clusters formation in CaF_2:Mn and CaF_2:Eu luminophors. Tartu, 2007, 100 p.
69. **Iiris Kahn**. Quantitative Structure-Activity Relationships of environmentally relevant properties. Tartu, 2007, 98 p.
70. **Mari Reinik.** Nitrates, nitrites, N-nitrosamines and polycyclic aromatic hydrocarbons in food: analytical methods, occurrence and dietary intake. Tartu, 2007, 172 p.
71. **Heili Kasuk.** Thermodynamic parameters and adsorption kinetics of organic compounds forming the compact adsorption layer at Bi single crystal electrodes. Tartu, 2007, 212 p.
72. **Erki Enkvist.** Synthesis of adenosine-peptide conjugates for biological applications. Tartu, 2007, 114 p.
73. **Svetoslav Hristov Slavov**. Biomedical applications of the QSAR approach. Tartu, 2007, 146 p.
74. **Eneli Härk.** Electroreduction of complex cations on electrochemically polished Bi(*hkl*) single crystal electrodes. Tartu, 2008, 158 p.
75. **Priit Möller.** Electrochemical characteristics of some cathodes for medium temperature solid oxide fuel cells, synthesized by solid state reaction technique. Tartu, 2008, 90 p.
76. **Signe Viggor.** Impact of biochemical parameters of genetically different pseudomonads at the degradation of phenolic compounds. Tartu, 2008, 122 p.
77. **Ave Sarapuu.** Electrochemical reduction of oxygen on quinone-modified carbon electrodes and on thin films of platinum and gold. Tartu, 2008, 134 p.
78. **Agnes Kütt.** Studies of acid-base equilibria in non-aqueous media. Tartu, 2008, 198 p.
79. **Rouvim Kadis.** Evaluation of measurement uncertainty in analytical chemistry: related concepts and some points of misinterpretation. Tartu, 2008, 118 p.
80. **Valter Reedo.** Elaboration of IVB group metal oxide structures and their possible applications. Tartu, 2008, 98 p.
81. **Aleksei Kuznetsov.** Allosteric effects in reactions catalyzed by the cAMP-dependent protein kinase catalytic subunit. Tartu, 2009, 133 p.

82. **Aleksei Bredihhin.** Use of mono- and polyanions in the synthesis of multisubstituted hydrazine derivatives. Tartu, 2009, 105 p.
83. **Anu Ploom.** Quantitative structure-reactivity analysis in organosilicon chemistry. Tartu, 2009, 99 p.
84. **Argo Vonk.** Determination of adenosine A_{2A}- and dopamine D_1 receptor-specific modulation of adenylate cyclase activity in rat striatum. Tartu, 2009, 129 p.
85. **Indrek Kivi.** Synthesis and electrochemical characterization of porous cathode materials for intermediate temperature solid oxide fuel cells. Tartu, 2009, 177 p.
86. **Jaanus Eskusson.** Synthesis and characterisation of diamond-like carbon thin films prepared by pulsed laser deposition method. Tartu, 2009, 117 p.
87. **Marko Lätt.** Carbide derived microporous carbon and electrical double layer capacitors. Tartu, 2009, 107 p.
88. **Vladimir Stepanov.** Slow conformational changes in dopamine transporter interaction with its ligands. Tartu, 2009, 103 p.
89. **Aleksander Trummal.** Computational Study of Structural and Solvent Effects on Acidities of Some Brønsted Acids. Tartu, 2009, 103 p.
90. **Eerold Vellemäe.** Applications of mischmetal in organic synthesis. Tartu, 2009, 93 p.
91. **Sven Parkel.** Ligand binding to 5-HT_{1A} receptors and its regulation by Mg^{2+} and Mn^{2+}. Tartu, 2010, 99 p.
92. **Signe Vahur.** Expanding the possibilities of ATR-FT-IR spectroscopy in determination of inorganic pigments. Tartu, 2010, 184 p.
93. **Tavo Romann**. Preparation and surface modification of bismuth thin film, porous, and microelectrodes. Tartu, 2010, 155 p.
94. **Nadežda Aleksejeva.** Electrocatalytic reduction of oxygen on carbon nanotube-based nanocomposite materials. Tartu, 2010, 147 p.
95. **Marko Kullapere.** Electrochemical properties of glassy carbon, nickel and gold electrodes modified with aryl groups. Tartu, 2010, 233 p.
96. **Liis Siinor.** Adsorption kinetics of ions at Bi single crystal planes from aqueous electrolyte solutions and room-temperature ionic liquids. Tartu, 2010, 101 p.
97. **Angela Vaasa.** Development of fluorescence-based kinetic and binding assays for characterization of protein kinases and their inhibitors. Tartu 2010, 101 p.
98. **Indrek Tulp.** Multivariate analysis of chemical and biological properties. Tartu 2010, 105 p.
99. **Aare Selberg.** Evaluation of environmental quality in Northern Estonia by the analysis of leachate. Tartu 2010, 117 p.
100. **Darja Lavõgina.** Development of protein kinase inhibitors based on adenosine analogue-oligoarginine conjugates. Tartu 2010, 248 p.
101. **Laura Herm.** Biochemistry of dopamine D_2 receptors and its association with motivated behaviour. Tartu 2010, 156 p.

102. **Terje Raudsepp.** Influence of dopant anions on the electrochemical properties of polypyrrole films. Tartu 2010, 112 p.
103. **Margus Marandi.** Electroformation of Polypyrrole Films: *In-situ* AFM and STM Study. Tartu 2011, 116 p.
104. **Kairi Kivirand.** Diamine oxidase-based biosensors: construction and working principles. Tartu, 2011, 140 p.
105. **Anneli Kruve.** Matrix effects in liquid-chromatography electrospray mass-spectrometry. Tartu, 2011, 156 p.
106. **Gary Urb.** Assessment of environmental impact of oil shale fly ash from PF and CFB combustion. Tartu, 2011, 108 p.
107. **Nikita Oskolkov.** A novel strategy for peptide-mediated cellular delivery and induction of endosomal escape. Tartu, 2011, 106 p.
108. **Dana Martin.** The QSPR/QSAR approach for the prediction of properties of fullerene derivatives. Tartu, 2011, 98 p.
109. **Säde Viirlaid.** Novel glutathione analogues and their antioxidant activity. Tartu, 2011, 106 p.
110. **Ülis Sõukand.** Simultaneous adsorption of Cd^{2+}, Ni^{2+}, and Pb^{2+} on peat. Tartu, 2011, 124 p.
111. **Lauri Lipping.** The acidity of strong and superstrong Brønsted acids, an outreach for the "limits of growth": a quantum chemical study. Tartu, 2011, 124 p.
112. **Heisi Kurig.** Electrical double-layer capacitors based on ionic liquids as electrolytes. Tartu, 2011, 146 p.
113. **Marje Kasari.** Bisubstrate luminescent probes, optical sensors and affinity adsorbents for measurement of active protein kinases in biological samples. Tartu, 2012, 126 p.
114. **Kalev Takkis.** Virtual screening of chemical databases for bioactive molecules. Tartu, 2012, 122 p.
115. **Ksenija Kisseljova**. Synthesis of aza-β^3-amino acid containing peptides and kinetic study of their phosphorylation by protein kinase A. Tartu, 2012, 104 p.
116. **Riin Rebane.** Advanced method development strategy for derivatization LC/ESI/MS. Tartu, 2012, 184 p.
117. **Vladislav Ivaništšev.** Double layer structure and adsorption kinetics of ions at metal electrodes in room temperature ionic liquids. Tartu, 2012, 128 p.
118. **Irja Helm.** High accuracy gravimetric Winkler method for determination of dissolved oxygen. Tartu, 2012, 139 p.
119. **Karin Kipper.** Fluoroalcohols as Components of LC-ESI-MS Eluents: Usage and Applications. Tartu, 2012, 164 p.
120. **Arno Ratas.** Energy storage and transfer in dosimetric luminescent materials. Tartu, 2012, 163 p.
121. **Reet Reinart-Okugbeni**. Assay systems for characterisation of subtype-selective binding and functional activity of ligands on dopamine receptors. Tartu, 2012, 159 p.

122. **Lauri Sikk.** Computational study of the Sonogashira cross-coupling reaction. Tartu, 2012, 81 p.
123. **Karita Raudkivi.** Neurochemical studies on inter-individual differences in affect-related behaviour of the laboratory rat. Tartu, 2012, 161 p.
124. **Indrek Saar.** Design of GalR2 subtype specific ligands: their role in depression-like behavior and feeding regulation. Tartu, 2013, 126 p.
125. **Ann Laheäär.** Electrochemical characterization of alkali metal salt based non-aqueous electrolytes for supercapacitors. Tartu, 2013, 127 p.
126. **Kerli Tõnurist.** Influence of electrospun separator materials properties on electrochemical performance of electrical double-layer capacitors. Tartu, 2013, 147 p.
127. **Kaija Põhako-Esko.** Novel organic and inorganic ionogels: preparation and characterization. Tartu, 2013, 124 p.
128. **Ivar Kruusenberg.** Electroreduction of oxygen on carbon nanomaterial-based catalysts. Tartu, 2013, 191 p.
129. **Sander Piiskop.** Kinetic effects of ultrasound in aqueous acetonitrile solutions. Tartu, 2013, 95 p.
130. **Ilona Faustova**. Regulatory role of L-type pyruvate kinase N-terminal domain. Tartu, 2013, 109 p.
131. **Kadi Tamm.** Synthesis and characterization of the micro-mesoporous anode materials and testing of the medium temperature solid oxide fuel cell single cells. Tartu, 2013, 138 p.
132. **Iva Bozhidarova Stoyanova-Slavova.** Validation of QSAR/QSPR for regulatory purposes. Tartu, 2013, 109 p.
133. **Vitali Grozovski**. Adsorption of organic molecules at single crystal electrodes studied by *in situ* STM method. Tartu, 2014, 146 p.
134. **Santa Veikšina**. Development of assay systems for characterisation of ligand binding properties to melanocortin 4 receptors. Tartu, 2014, 151 p.
135. **Jüri Liiv.** PVDF (polyvinylidene difluoride) as material for active element of twisting-ball displays. Tartu, 2014, 111 p.
136. **Kersti Vaarmets.** Electrochemical and physical characterization of pristine and activated molybdenum carbide-derived carbon electrodes for the oxygen electroreduction reaction. Tartu, 2014, 131 p.
137. **Lauri Tõntson**. Regulation of G-protein subtypes by receptors, guanine nucleotides and Mn^{2+}. Tartu, 2014, 105 p.
138. **Aiko Adamson.** Properties of amine-boranes and phosphorus analogues in the gas phase. Tartu, 2014, 78 p.
139. **Elo Kibena**. Electrochemical grafting of glassy carbon, gold, highly oriented pyrolytic graphite and chemical vapour deposition-grown graphene electrodes by diazonium reduction method. Tartu, 2014, 184 p.
140. **Teemu Näykki.** Novel Tools for Water Quality Monitoring – From Field to Laboratory. Tartu, 2014, 202 p.
141. **Karl Kaupmees.** Acidity and basicity in non-aqueous media: importance of solvent properties and purity. Tartu, 2014, 128 p.

142. **Oleg Lebedev**. Hydrazine polyanions: different strategies in the synthesis of heterocycles. Tartu, 2015, 118 p.
143. **Geven Piir.** Environmental risk assessment of chemicals using QSAR methods. Tartu, 2015, 123 p.
144. **Olga Mazina.** Development and application of the biosensor assay for measurements of cyclic adenosine monophosphate in studies of G protein-coupled receptor signalinga. Tartu, 2015, 116 p.
145. **Sandip Ashokrao Kadam.** Anion receptors: synthesis and accurate binding measurements. Tartu, 2015, 116 p.
146. **Indrek Tallo.** Synthesis and characterization of new micro-mesoporous carbide derived carbon materials for high energy and power density electrical double layer capacitors. Tartu, 2015, 148 p.
147. **Heiki Erikson.** Electrochemical reduction of oxygen on nanostructured palladium and gold catalysts. Tartu, 2015, 204 p.
148. **Erik Anderson.** *In situ* Scanning Tunnelling Microscopy studies of the interfacial structure between Bi(111) electrode and a room temperature ionic liquid. Tartu, 2015, 118 p.
149. **Girinath G. Pillai.** Computational Modelling of Diverse Chemical, Biochemical and Biomedical Properties. Tartu, 2015, 140 p.
150. **Piret Pikma.** Interfacial structure and adsorption of organic compounds at Cd(0001) and Sb(111) electrodes from ionic liquid and aqueous electrolytes: an *in situ* STM study. Tartu, 2015, 126 p.
151. **Ganesh babu Manoharan.** Combining chemical and genetic approaches for photoluminescence assays of protein kinases. Tartu, 2016, 126 p.
152. **Carolin Siimenson**. Electrochemical characterization of halide ion adsorption from liquid mixtures at Bi(111) and pyrolytic graphite electrode surface. Tartu, 2016, 110 p.
153. **Asko Laaniste.** Comparison and optimisation of novel mass spectrometry ionisation sources. Tartu, 2016, 156 p.
154. **Hanno Evard.** Estimating limit of detection for mass spectrometric analysis methods. Tartu, 2016, 224 p.
155. **Kadri Ligi.** Characterization and application of protein kinase-responsive organic probes with triplet-singlet energy transfer. Tartu, 2016, 122 p.
156. **Margarita Kagan.** Biosensing penicillins' residues in milk flows. Tartu, 2016, 130 p.
157. **Marie Kriisa.** Development of protein kinase-responsive photoluminescent probes and cellular regulators of protein phosphorylation. Tartu, 2016, 106 p.
158. **Mihkel Vestli.** Ultrasonic spray pyrolysis deposited electrolyte layers for intermediate temperature solid oxide fuel cells. Tartu, 2016, 156 p.
159. **Silver Sepp**. Influence of porosity of the carbide-derived carbon on the properties of the composite electrocatalysts and characteristics of polymer electrolyte fuel cells. Tartu, 2016, 137 p.
160. **Kristjan Haav**. Quantitative relative equilibrium constant measurements in supramolecular chemistry. Tartu, 2017, 158 p.

161. **Anu Teearu**. Development of MALDI-FT-ICR-MS methodology for the analysis of resinous materials. Tartu, 2017, 205 p.
162. **Taavi Ivan**. Bifunctional inhibitors and photoluminescent probes for studies on protein complexes. Tartu, 2017, 140 p.
163. **Maarja-Liisa Oldekop**. Characterization of amino acid derivatization reagents for LC-MS analysis. Tartu, 2017, 147 p.
164. **Kristel Jukk**. Electrochemical reduction of oxygen on platinum- and palladium-based nanocatalysts. Tartu, 2017, 250 p.
165. **Siim Kukk**. Kinetic aspects of interaction between dopamine transporter and *N*-substituted nortropane derivatives. Tartu, 2017, 107 p.
166. **Birgit Viira**. Design and modelling in early drug development in targeting HIV-1 reverse transcriptase and Malaria. Tartu, 2017, 172 p.
167. **Rait Kivi**. Allostery in cAMP dependent protein kinase catalytic subunit. Tartu, 2017, 115 p.
168. **Agnes Heering**. Experimental realization and applications of the unified acidity scale. Tartu, 2017, 123 p.
169. **Delia Juronen**. Biosensing system for the rapid multiplex detection of mastitis-causing pathogens in milk. Tartu, 2018, 85 p.
170. **Hedi Rahnel.** ARC-inhibitors: from reliable biochemical assays to regulators of physiology of cells. Tartu, 2018, 176 p.
171. **Anton Ruzanov.** Computational investigation of the electrical double layer at metal–aqueous solution and metal–ionic liquid interfaces. Tartu, 2018, 129 p.
172. **Katrin Kestav.** Crystal Structure-Guided Development of Bisubstrate-Analogue Inhibitors of Mitotic Protein Kinase Haspin. Tartu, 2018, 166 p.
173. **Mihkel Ilisson.** Synthesis of novel heterocyclic hydrazine derivatives and their conjugates. Tartu, 2018, 101 p.
174. **Anni Allikalt.** Development of assay systems for studying ligand binding to dopamine receptors. Tartu, 2018, 160 p.
175. **Ove Oll.** Electrical double layer structure and energy storage characteristics of ionic liquid based capacitors. Tartu, 2018, 187 p.
176. **Rasmus Palm.** Carbon materials for energy storage applications. Tartu, 2018, 114 p.
177. **Jörgen Metsik.** Preparation and stability of poly(3,4-ethylenedioxythiophene) thin films for transparent electrode applications. Tartu, 2018, 111 p.
178. **Sofja Tšepelevitš.** Experimental studies and modeling of solute-solvent interactions. Tartu, 2018, 109 p.
179. **Märt Lõkov.** Basicity of some nitrogen, phosphorus and carbon bases in acetonitrile. Tartu, 2018, 104 p.
180. **Anton Mastitski**. Preparation of α-aza-amino acid precursors and related compounds by novel methods of reductive one-pot alkylation and direct alkylation. Tartu, 2018, 155 p.
181. **Jürgen Vahter**. Development of bisubstrate inhibitors for protein kinase CK2. Tartu, 2019, 186 p.

182. **Piia Liigand.** Expanding and improving methodology and applications of ionization efficiency measurements. Tartu, 2019, 189 p.
183. **Sigrid Selberg.** Synthesis and properties of lipophilic phosphazene-based indicator molecules. Tartu, 2019, 74 p.
184. **Jaanus Liigand.** Standard substance free quantification for LC/ESI/MS analysis based on the predicted ionization efficiencies. Tartu, 2019, 254 p.
185. **Marek Mooste.** Surface and electrochemical characterisation of aryl film and nanocomposite material modified carbon and metal-based electrodes. Tartu, 2019, 304 p.
186. **Mare Oja.** Experimental investigation and modelling of pH profiles for effective membrane permeability of drug substances. Tartu, 2019, 306 p.
187. **Sajid Hussain.** Electrochemical reduction of oxygen on supported Pt catalysts. Tartu, 2019, 220 p.
188. **Ronald Väli.** Glucose-derived hard carbon electrode materials for sodium-ion batteries. Tartu, 2019, 180 p.
189. **Ester Tee.** Analysis and development of selective synthesis methods of hierarchical micro- and mesoporous carbons. Tartu, 2019, 210 p.
190. **Martin Maide.** Influence of the microstructure and chemical composition of the fuel electrode on the electrochemical performance of reversible solid oxide fuel cell. Tartu, 2020, 144 p.
191. **Edith Viirlaid.** Biosensing Pesticides in Water Samples. Tartu, 2020, 102 p.
192. **Maike Käärik.** Nanoporous carbon: the controlled nanostructure, and structure-property relationships. Tartu, 2020, 162 p.
193. **Artur Gornischeff.** Study of ionization efficiencies for derivatized compounds in LC/ESI/MS and their application for targeted analysis. Tartu, 2020, 124 p.
194. **Reet Link.** Ligand binding, allosteric modulation and constitutive activity of melanocortin-4 receptors. Tartu, 2020, 108 p.
195. **Pilleriin Peets.** Development of instrumental methods for the analysis of textile fibres and dyes. Tartu, 2020, 150 p.
196. **Larisa Ivanova.** Design of active compounds against neurodegenerative diseases. Tartu, 2020, 152 p.
197. **Meelis Härmas.** Impact of activated carbon microstructure and porosity on electrochemical performance of electrical double-layer capacitors. Tartu, 2020, 122 p.
198. **Ruta Hecht.** Novel Eluent Additives for LC-MS Based Bioanalytical Methods. Tartu, 2020, 202 p.
199. **Max Hecht.** Advances in the Development of a Point-of-Care Mass Spectrometer Test. Tartu, 2020, 168 p.
200. **Ida Rahu.** Bromine formation in inorganic bromide/nitrate mixtures and its application for oxidative aromatic bromination. Tartu, 2020, 116 p.
201. **Sander Ratso**. Electrocatalysis of oxygen reduction on non-precious metal catalysts. Tartu, 2020, 371 p.
202. **Astrid Darnell.** Computational design of anion receptors and evaluation of host-guest binding. Tartu, 2021, 150 p.

203. **Ove Korjus.** The development of ceramic fuel electrode for solid oxide cells. Tartu, 2021, 150 p.
204. **Merit Oss.** Ionization efficiency in electrospray ionization source and its relations to compounds' physico-chemical properties. Tartu, 2021, 124 p.
205. **Madis Lüsi**. Electroreduction of oxygen on nanostructured palladium catalysts. Tartu, 2021, 180 p.